Fri. Sep 6, 2019

Hall A

Oral Session | Food Function/Nutrition

[6-1015-A] Functional/Wellness Foods &Nutrition (2)

Chair:Rungarun Sasanatayart(Mae Fah Luang University, Thailand)
10:15 AM - 11:30 AM Hall A (Main Hall)

[6-1015-A-01] **Change of Bioactive Compounds and Bioactivities of Crisphead Lettuce during Simulated *In Vitro* Digestion**
*Sunantha Ketnawa[1], Yukiharu Ogawa[1] (1. Graduate School of Horticulture, Chiba University(Japan))
10:15 AM - 10:30 AM

[6-1015-A-02] **Impact of Crystallinity Change During *In Vitro* Digestion on Starch Digestibility of Microwave- and Steam-Cooked Black Rice**
*Sukanya Thuengtung[1], Yoshitaka Matsushita[2], Yukiharu Ogawa[1] (1. Graduate School of Horticulture, Chiba University(Japan), 2. Research Network and Facility Services Division, National Institute for Materials Science (NIMS)(Japan))
10:30 AM - 10:45 AM

[6-1015-A-03] **Study of Static *In Vitro* Digestion of Japanese Pickled Plums on the Change of Polyphenols and Antioxidant Activity**
*Jutalak Suwannachot[1], Sunantha Ketnawa[1], Yukiharu Ogawa[1] (1. Chiba University(Japan))
10:45 AM - 11:00 AM

[6-1015-A-04] **Preparation of Pigment Extract Loaded Alginate Beads and Their Stability of Antioxidant Activities during *in vitro* Gastrointestinal Digestion**
*Rungarun Sasanatayart[1], Sutthiwal Setha[1] (1. School of Agro-Industry, Mae Fah Luang University(Thailand))
11:00 AM - 11:15 AM

[6-1015-A-05] **Stability of Plant Pigments and Antioxidant Activities in Juice Model during Processing and *in vitro* Gastrointestinal Digestion**
*Titikan Liangpanth[1], Rungarun Sasanatayart[1] (1. School of Agro-Industry, Mae Fah Luang University(Thailand))
11:15 AM - 11:30 AM

Room C

Oral Session | Postharvest/Food Technology and Process Engineering

[6-1015-C] Postharvest/Food Technology and Process Engineering (6)

Chair:Xujun Ye(Hirosaki University, Japan)
10:15 AM - 11:30 AM Room C (3rd room)

[6-1015-C-01] **Spatially Resolved Interactance Spectroscopy to Estimate Degree of Red Coloration in Red-fleshed Apple Cultivar 'Kurenai-no-Yume'**
*Xujun Ye[1], Sou Takada[1], Shuhuai Zhang[1] (1. Hirosaki University(Japan))
10:15 AM - 10:30 AM

[6-1015-C-02] **Use of hyperspectral imaging to separate cultivars and evaluate the internal quality of nectarines**
Sandra Munera[1], Prieto Andres[1], Nuria Aleixos[2], Sergio Cubero[1], *Jose Blasco[1] (1. Centro de Agroingeniería. Instituto Valenciano de Investigaciones Agrarias (IVIA). Ctra. Moncada-Náquera Km 4.5, 46113, Moncada, Valencia(Spain), 2. Departamento de Ingeniería Gráfica. Universitat Politècnica de València. Camino de Vera, s/n, 46022 Valencia(Spain))
10:30 AM - 10:45 AM

[6-1015-C-03] **Evaluating the Performance of Unmanned Crop Sensing Robot for Rice**
*Dhirendranath Singh[1], Shigeru Ichiura[1], Mitsuhiko Katahira[2,1] (1. United Graduate School of Agriculture , Iwate University(Japan), 2. Faculty of Agriculture, Yamagata University(Japan))
10:45 AM - 11:00 AM

[6-1015-C-04] **Application of Non-destructive Determination of Rice Amylose Content at Grain Elevators**
*Edenio Olivares Diaz[1], Shuso Kawamura[1], Miki Matsuo[1], Toru Nagata[2], Shigenobu Koseki[1] (1. Hokkaido University(Japan), 2. Hokkaido Research Organization Central Agricultural Experiment Station(Japan))
11:00 AM - 11:15 AM

[6-1015-C-05] **Cow Milk Progesterone Concentration**

Determination during Milking Using Near-infrared Spectroscopy

*Patricia Nneka Iweka[1], Shuso Kawamura[1], Tomohiro Mitani[2], Takashi Kawaguchi[3], Shigenobu Koseki[1] （1. Hokkaido Univ.(Japan), 2. Field Sc. Center(Japan), 3. Orion Mach.(Japan)）

11:15 AM - 11:30 AM

Room D

Oral Session | Others (including the category of JSAM and SASJ)

[6-1015-D] Other Categories (3)

Chair:Takahiro Orikasa(Iwate University, Japan)
10:15 AM - 11:30 AM Room D (4th room)

[6-1015-D-01] **Field Representation and Path Planning for Robot Tractors**

*Hao Wang[1], Noboru Noguchi[1] （1. Hokkaido University(Japan)）

10:15 AM - 10:30 AM

[6-1015-D-02] **Driving Force Control for Suppression of Tractor’ s Dynamic Pitching Angle**

*Yuya Aoyagi[1], Masami Matsui[2] （1. Tokyo University of Agriculture and Technology (Japan), 2. Utsunomiya University(Japan)）

10:30 AM - 10:45 AM

[6-1015-D-03] **Development of a Smart Spraying System For Weeds On Rice Fields**

*Thanh Tinh Nguyen[1], Ricardo Ospina[2], Noboru Noguchi[2] （1. Hokkaido University, Graduate School of Agriculture(Japan), 2. Hokkaido University, Research Faculty of Agriculture(Japan)）

10:45 AM - 11:00 AM

[6-1015-D-04] **Deep Learning and Multiple Sensors Data Acquisition System for Real-time Decision Analysis in Agriculture Using Unmanned Aerial Vehicle**

*Yunyan Xie[1], Ryozo Noguchi[2], Tofael Ahamed[2] （1. Graduate School of Life and Environmental Sciences, University of Tsukuba(Japan), 2. Faculty of Life and Environmental Sciences, University of Tsukuba(Japan)）

11:00 AM - 11:15 AM

[6-1015-D-05] **Autonomous Navigation and Obstacle Avoidance for a Robotic Mower using Machine Vision**

*Kosuke Inoue[1] （1. The University of Tokyo(Japan)）

11:15 AM - 11:30 AM

Oral Session | Food Function/Nutrition

[6-1015-A] Functional/Wellness Foods &Nutrition (2)

Chair:Rungarun Sasanatayart(Mae Fah Luang University, Thailand)

Fri. Sep 6, 2019 10:15 AM - 11:30 AM Hall A (Main Hall)

[6-1015-A-01] Change of Bioactive Compounds and Bioactivities of Crisphead Lettuce during Simulated *In Vitro* Digestion

*Sunantha Ketnawa[1], Yukiharu Ogawa[1] （1. Graduate School of Horticulture, Chiba University(Japan)）

10:15 AM - 10:30 AM

[6-1015-A-02] Impact of Crystallinity Change During *In Vitro* Digestion on Starch Digestibility of Microwave- and Steam-Cooked Black Rice

*Sukanya Thuengtung[1], Yoshitaka Matsushita[2], Yukiharu Ogawa[1] （1. Graduate School of Horticulture, Chiba University(Japan), 2. Research Network and Facility Services Division, National Institute for Materials Science (NIMS)(Japan)）

10:30 AM - 10:45 AM

[6-1015-A-03] Study of Static *In Vitro* Digestion of Japanese Pickled Plums on the Change of Polyphenols and Antioxidant Activity

*Jutalak Suwannachot[1], Sunantha Ketnawa[1], Yukiharu Ogawa[1] （1. Chiba University(Japan)）

10:45 AM - 11:00 AM

[6-1015-A-04] Preparation of Pigment Extract Loaded Alginate Beads and Their Stability of Antioxidant Activities during *in vitro* Gastrointestinal Digestion

*Rungarun Sasanatayart[1], Sutthiwal Setha[1] （1. School of Agro-Industry, Mae Fah Luang University(Thailand)）

11:00 AM - 11:15 AM

[6-1015-A-05] Stability of Plant Pigments and Antioxidant Activities in Juice Model during Processing and *in vitro* Gastrointestinal Digestion

*Titikan Liangpanth[1], Rungarun Sasanatayart[1] （1. School of Agro-Industry, Mae Fah Luang University(Thailand)）

11:15 AM - 11:30 AM

Oral Session | Food Function/Nutrition
[6-1015-A] Functional/Wellness Foods &Nutrition (2)
Fri. Sep 6, 2019 10:15 AM - 11:30 AM Hall A (Main Hall)

[6-1015-A-01] Change of Bioactive Compounds and Bioactivities of Crisphead Lettuce during Simulated *In Vitro* Digestion

*Sunantha Ketnawa[1], Yukiharu Ogawa[1] (1. Graduate School of Horticulture, Chiba University(Japan))
Keywords: In vitro digestion, crisphead lettuce, bioactive compounds, bioactivity, bioaccessibility

Lettuces (*Lactuca sativa* L.) are the most popular vegetables in the world and are consumed in increasing amounts due to a good contribution to human health. Favorite species are butterhead, romaine, and, most importantly, crisphead (iceberg) lettuce. Crisphead lettuce is also of particular interest due to its high content in antioxidants and phytochemicals including caffeic acid and its derivatives, flavonols, vitamins C and E, chlorophyll, and carotenoids. The potential health benefit of crisphead lettuce before and after the simulated *in vitro* digestion will be represented by the recovery, bioaccessibility, and change of bioactive compounds [including total phenolic (TPC) and total flavonoids content (TFC)] and bioactivities [*in vitro* antioxidant activities including 2,2-diphenyl-1-picrylhydrazyl (DPPH), 2, 2’ -azinobis-(3-ethylbenzothiazoline-6-sulfonic acid) (ABTS) radical scavenging activities, ferric reducing antioxidant power (FRAP) and metal ion chelating (MIC)]. Thus, the objectives of this study were to study the change on recovery and bioaccessibility of those properties of cripshead lettuce utilizing simulated *in vitro* digestion model. The results suggest that the releasing of bioactive compounds as well as bioactivities increased during gastric digestion and intestinal digestion for 1 h then decreased when IVD completed, thus coordinated with recovery and bioaccessibility index. Crisphead lettuce showed the highest recovery and bioaccessibility of TPC and TFC at gastric phase digestion for more than 60% and 70%, respectively whereas the lowest of those found in after finish digestion for around 50% for both TPC and TFC. Among all bioactivities, crisphead lettuce sample showed the recovery and bioaccesibility of ABTS (61-92%) followed by FRAP (71-84%), DPPH (24-52%) and MIC (21-46%) during the digestion. The present study suggests that cripshead lettuce maintains stability in both bioactive compound and bioactivities during the digestion. Regarding the 4 methods used, significant correlations were found between bioactive compounds and antioxidant activity while ABTS exhibited weaker with TFC than TPC. Taken together, a relatively tight coupling of four parameters indicates that every one of them can be considered as a relevant and reliable characteristic of the antioxidant capacity of lettuce. This would provide a scientific basis for further studies on develop formulating new functional foods due to high nutritional value tolerant.

Change of Bioactive Compounds and Bioactivities of Crisphead Lettuce during Simulated *In Vitro* Digestion

Sunantha Ketnawa and Yukiharu Ogawa

Graduate School of Horticulture, Chiba University, 648, Matsudo, Matsudo 271-8510, Japan

*Corresponding author: ogwy@faculty.chiba-u.jp

ABSTRACT

Lettuces (*Lactuca sativa* L.) are the most popular vegetables in the world and are consumed in increasing amounts due to a good contribution to human health. Favorite species are butterhead, romaine, and, most importantly, crisphead (iceberg) lettuce. Crisphead lettuce is also of particular interest due to its high content in antioxidants and phytochemicals including caffeic acid and its derivatives, flavonols, vitamins C and E, chlorophyll, and carotenoids. The potential health benefit of crisphead lettuce before and after the simulated *in vitro* digestion will be represented by the recovery, bioaccessibility, and change of bioactive compounds [including total phenolic (TPC) and total flavonoids content (TFC)] and bioactivities [*in vitro* antioxidant activities including 2,2-diphenyl-1-picrylhydrazyl (DPPH), 2, 2'-azinobis-(3-ethylbenzothiazoline-6-sulfonic acid) (ABTS) radical scavenging activities, ferric reducing antioxidant power (FRAP) and metal ion chelating (MIC)]. Thus, the objectives of this study were to study the change on recovery and bioaccessibility of those properties of cripshead lettuce utilizing simulated *in vitro* digestion model. The results suggest that the releasing of bioactive compounds as well as bioactivities increased during gastric digestion and intestinal digestion for 1 h then decreased when IVD completed, thus coordinated with recovery and bioaccessibility index. Crisphead lettuce showed the highest recovery and bioaccessibility of TPC and TFC at gastric phase digestion for more than 60% and 70%, respectively whereas the lowest of those found in after finish digestion for around 50% for both TPC and TFC. Among all bioactivities, crisphead lettuce sample showed the recovery and bioaccesibility of ABTS (61-92%) followed by FRAP (71-84%), DPPH (24-52%) and MIC (21-46%) during the digestion. The present study suggests that cripshead lettuce maintains stability in both bioactive compound and bioactivities during the digestion. Regarding the 4 methods used, significant correlations were found between bioactive compounds and antioxidant activity while ABTS exhibited weaker with TFC than TPC. Taken together, a relatively tight coupling of four parameters indicates that every one of them can be considered as a relevant and reliable characteristic of the antioxidant capacity of lettuce. This would provide a scientific basis for further studies on develop formulating new functional foods due to high nutritional value tolerant.

Keywords: *In vitro* digestion, crisphead lettuce, bioactive compounds, bioactivity. bioaccessibility

10:30 AM - 10:45 AM (Fri. Sep 6, 2019 10:15 AM - 11:30 AM Hall A)

[6-1015-A-02] Impact of Crystallinity Change During *In Vitro* Digestion on Starch Digestibility of Microwave- and Steam-Cooked Black Rice

*Sukanya Thuengtung[1], Yoshitaka Matsushita[2], Yukiharu Ogawa[1] (1. Graduate School of Horticulture, Chiba University(Japan), 2. Research Network and Facility Services Division, National Institute for Materials Science (NIMS)(Japan))

Keywords: Black rice, Crystallinity, Microwave-cooking, Steam-cooking, Starch digestibility, X-ray diffraction

Rice is a major cereal crop that is consumed as staple food by around half of the world' s population. Rice can be distinguished by the color of grain' s pericarp layer, as pigmented and non-pigmented rice. Black pigmented rice has been long cultivated in Southeast Asian countries, and has received much attention due to its nutritional values. Carbohydrate is known as a major macronutrient of rice that could be accounted as starch content for 90%. Starch digestion is a complex process that occurs mainly in the small intestine. Several factors could influence the starch digestibility such as starch granule structure, particle size, and food processing. Consequently, the effect of microwave and steam-cooking on change of crystallinity during *in vitro* digestion, including their impact on starch digestibility of black rice were examined. Influence of rice attribute on starch digestibility was also investigated. In this study, unpolished Thai black rice (cv. Hom Nin) was soaked at 10 º C for 19 h before cooked by microwave and steam methods for 12 and 25 min, respectively. No white core inside cooked rice grain indicated full gelatinization. A portion of cooked black rice grain was ground to obtain homogenized slurry sample. Intact rice grain and homogenized slurry samples were then transferred into each *in vitro* reactor to start the simulated digestion. There were two digestion states included simulated gastric and simulated small intestinal digestion, which the supernatant was collected during these digestive states to analyze hydrolysis of starch. In addition, rice grain samples of uncooked rice, and cooked rice before and during *in vitro* digestion, were collected and prepared as the rice flour for analysis of X-ray diffraction (XRD) pattern. The results revealed that XRD pattern of uncooked black rice exhibited the diffraction peak at 15, 17, 18, and 23º (2θ), indicating A-type crystalline structure. However, XRD pattern was changed after cooking which diffraction peak was found at 13 and 20º (2θ), indicating V_h-type crystalline structure. Moreover, XRD pattern and the degree of crystallinity of steam-cooked rice were outstandingly changed after 360 and 480 min of simulated small intestinal digestion, comparing to microwave-cooked rice. The equilibrium starch hydrolysis (C_∞) percentage of steam-cooked rice showed lower than that of microwave-cooked rice as well. Besides, structure-less of homogenized slurry sample influenced faster starch hydrolysis rate when compared with intact grain sample. This study implied that rice attribute has an impact on starch hydrolysis rate of black rice, which different C_∞ between two cooking methods could be involved with change of the crystallinity degree during *in vitro* digestion.

10:45 AM - 11:00 AM (Fri. Sep 6, 2019 10:15 AM - 11:30 AM Hall A)

[6-1015-A-03] Study of Static *In Vitro* Digestion of Japanese Pickled Plums on the Change of Polyphenols and Antioxidant Activity

*Jutalak Suwannachot[1], Sunantha Ketnawa[1], Yukiharu Ogawa[1] (1. Chiba University(Japan))

Keywords: Antioxidant activity, In vitro digestion, Pickled plum, Polyphenols

Japanese plum (Ume in Japanese; *Prunus mume*) is basically consumed in processed forms, e.g. a pickled and dried form (Umeboshi), liquored form (Umeshu), and concentrated form (Bainiku-ekisu). These products have been known to possess various medicinal benefits and have been frequently prescribed as a traditional folk medicine, owing to the fruit is a good source of organic acids, edible fiber, minerals, and phenolic compounds. Two types of pickled plums (PP) called kari-kari ume (hard type [HPP]) and umeboshi (soft type [SPP]) from commercial products in Japan were used and evaluated. These products are widely consumed with rice or processed to be puree and paste products. In this study, the static *in vitro* digestion was investigated with and without digestive enzymes (control [CT]) by sampling at undigested stage (G0), 1 hour after gastric digestion (G1), 1 hour after small intestinal digestion (G1I1) and 2 hours after small intestinal digestion (G1I2). The changes of polyphenols (total phenolics [TPC] and total flavonoid contents [TFC]) and antioxidant activities (DPPH- and ABTS-radical scavenging activities, ferric reducing antioxidant power [FRAP], and metal ion chelating [MIC] activity) were investigated during simulated *in vitro* gastrointestinal digestion. Increment of TPC and TFC was found during the simulated digestion in both of PP samples. In addition, higher antioxidant activities were found during simulated digestion of digested PP when compared to those of CT. Furthermore, higher ABTS and FRAP activities were observed in HPP during gastric stage than those SPP. Nevertheless, released antioxidant activities of SPP were better than those of HPP during the small intestinal stage, except MIC activity. Regarding the releasing of antioxidant activity may be related to cell structure. Thus, differences in the initial fruit maturity and production method of PP could enhance the releasing of antioxidant activities. In conclusion, these results provided information about developing new functional food products. Therefore, the study can be applied to develop a processing method to provide maximum bioactivity for the improvement of human well-being.

11:00 AM - 11:15 AM (Fri. Sep 6, 2019 10:15 AM - 11:30 AM Hall A)

[6-1015-A-04] Preparation of Pigment Extract Loaded Alginate Beads and Their Stability of Antioxidant Activities during *in vitro* Gastrointestinal Digestion

*Rungarun Sasanatayart[1], Sutthiwal Setha[1] （1. School of Agro-Industry, Mae Fah Luang University(Thailand)）

Keywords: Anthocyanins , Carotenoids , Antioxidant , Alginate based Encapsulation , in vitro gastrointestinal digestion

Plant pigments are safe for food applications and exert antioxidant activities, providing health benefits superior to synthetic colorants. However, there are challenges related to color losses during food processing, storage, and commercialization due to a low stability of natural pigments. In addition, based on human gastrointestinal digestion, levels of bioactive compounds and their related antioxidant activities are significantly altered. One effective approach to preserve the health beneficial properties of plant pigments is to incorporate them into polymer matrices for the improvement of stability and bioavailability. In this study, 2.5% w/w pigment extracted from butterfly pea flower (BPF) and 5% w/w pigment extracted from turmeric rhizome (TR) were prepared. PBF and TR loaded alginate beads were prepared by extrusion method using 1%w/v alginate and 2%w/v calcium chloride ($CaCl_2$). To examine the stability through simulated gastrointestinal digestion, a certain amount of BPF and TR loaded alginate beads were either added into distilled water or formulated into juice model samples containing 10%w/v glucose and 0.1M citric acid. To assess effect of heat, all samples were adjusted to pH 3.0 and were subjected to pasteurization at 75^{o}C for

15 min. Samples without heat treatment were also compared. Samples were examined for antioxidant properties in terms of total anthocyanins content (TAC) for BPF, total carotenoids content (TCC) for TR, total phenol content (TPC), total flavonoid content (TFC) and antioxidant activities based on FRAP and DPPH assays. During *in-vitro* gastrointestinal digestion, samples showed different amount and stability of TAC, TCC, TPC, TFC and antioxidant activities based on FRAP and DPPH, regarding type of pigments. Results showed that alginate-based encapsulation of pigment extract limited the release of bioactive compound during *in vitro* gastrointestinal digestion. The effect of either pasteurized heat alone or in combining with ingredients in releasing more bioactive components of juice model samples was also noted. During *in vitro* gastrointestinal digestion, the high stability of bioactive compounds and antioxidant activities from oral phase (G0) to gastric phase (G30) but subsequently lower stability along intestinal phase (I0-I120) were observed in all samples. These stability data supports the beneficial effect of alginate-based encapsulation in controlled releasing of bioactive compounds of plant pigments and their bioavailability which could be further applied in food industry.

11:15 AM - 11:30 AM (Fri. Sep 6, 2019 10:15 AM - 11:30 AM Hall A)

[6-1015-A-05] Stability of Plant Pigments and Antioxidant Activities in Juice Model during Processing and *in vitro* Gastrointestinal Digestion

*Titikan Liangpanth[1], Rungarun Sasanatayart[1] (1. School of Agro-Industry, Mae Fah Luang University(Thailand))

Keywords: Anthocyanins , Carotenoids , Betalains, Chlorophylls, in vitro gastrointestinal digestion, Antioxidant

Due to the changing perceptions of consumers to consume natural products, there is an increasing interest in the use of natural antioxidant pigments as substitutes for synthetic food colorants. Plant pigments exert antioxidant activities, providing health benefits. However, there are challenges related to color losses during food processing, storage, and commercialization due to a low stability of natural pigments compared to synthetic colorants. In this study, four pigment powders extracted from selected plant parts including butterfly pea flower rich in anthocyanins (TAC), dragon fruit peel containing betalains (TBC), turmeric rhizome containing curcuminoids (TCC) and pandan leaves rich in chlorophylls (TCPC) were compared. To examine the stability through processing, juice model samples containing 10% (w/v) glucose, 0.1M citric acid and coloring with 1.0-3.0% (w/v) color powder were prepared. The samples were adjusted to pH 3 and 7 and subjected to three different heat treatments including (1) No heat (control), pasteurization (75° C for 15 min) and sterilization (121° C for 15 min). All samples were measured for color parameters (L*, a*, b*, hue and Δ E) whilst, antioxidant properties were measured in terms of total phenol content (TPC) and antioxidant activities based on FRAP and DPPH assays. Results showed that pH and heat treatments played a critical role on stability of pigment compounds, resulting in change in visual color and color parameters which could limit food uses. Overall, pasteurization of juice model samples rich in plant pigments at both pH 3 and 7 was better than sterilization in retaining initial color and maximize level of bioactive compounds and related antioxidant properties. To assess stability and bioaccessibility of antioxidant properties during simulated *in-vitro* gastrointestinal digestion, all pasteurized juice model solutions at pH 3 were compared. During digestion, all juice model solutions showed different stability of pigments compound, TPC and antioxidant activities based on FRAP and DPPH. Overall, trends observed were the increased stability of bioactive compounds and their related antioxidant activities from oral phase (G0) to gastric phase (G30) but

subsequently decreased stability along intestinal phase (I0-I120). All pigment compounds, TAC, TBC, TCC and TCPC showed the less correlation with antioxidant activities based on FRAP and DPPH than did TPC. Results suggested that the concentration of pigment compounds and the antioxidant capacity before digestion might not reflect the after digested concentration. Data of this study provided relevant information on antioxidants reflecting stability and activity during digestion which supports the potential use of plant pigments in natural foods and beverages.

Oral Session | Postharvest/Food Technology and Process Engineering

[6-1015-C] Postharvest/Food Technology and Process Engineering (6)

Chair:Xujun Ye(Hirosaki University, Japan)

Fri. Sep 6, 2019 10:15 AM - 11:30 AM Room C (3rd room)

[6-1015-C-01] Spatially Resolved Interactance Spectroscopy to Estimate Degree of Red Coloration in Red-fleshed Apple Cultivar 'Kurenai-no-Yume'

*Xujun Ye[1], Sou Takada[1], Shuhuai Zhang[1] （1. Hirosaki University(Japan)）

10:15 AM - 10:30 AM

[6-1015-C-02] Use of hyperspectral imaging to separate cultivars and evaluate the internal quality of nectarines

Sandra Munera[1], Prieto Andres[1], Nuria Aleixos[2], Sergio Cubero[1], *Jose Blasco[1] （1. Centro de Agroingeniería. Instituto Valenciano de Investigaciones Agrarias (IVIA). Ctra. Moncada-Náquera Km 4.5, 46113, Moncada, Valencia(Spain), 2. Departamento de Ingeniería Gráfica. Universitat Politècnica de València. Camino de Vera, s/n, 46022 Valencia(Spain)）

10:30 AM - 10:45 AM

[6-1015-C-03] Evaluating the Performance of Unmanned Crop Sensing Robot for Rice

*Dhirendranath Singh[1], Shigeru Ichiura[1], Mitsuhiko Katahira[2,1] （1. United Graduate School of Agriculture , Iwate University(Japan), 2. Faculty of Agriculture, Yamagata University(Japan)）

10:45 AM - 11:00 AM

[6-1015-C-04] Application of Non-destructive Determination of Rice Amylose Content at Grain Elevators

*Edenio Olivares Diaz[1], Shuso Kawamura[1], Miki Matsuo[1], Toru Nagata[2], Shigenobu Koseki[1] （1. Hokkaido University(Japan), 2. Hokkaido Research Organization Central Agricultural Experiment Station(Japan)）

11:00 AM - 11:15 AM

[6-1015-C-05] Cow Milk Progesterone Concentration Determination during Milking Using Near-infrared Spectroscopy

*Patricia Nneka Iweka[1], Shuso Kawamura[1], Tomohiro Mitani[2], Takashi Kawaguchi[3], Shigenobu Koseki[1] （1. Hokkaido Univ.(Japan), 2. Field Sc. Center(Japan), 3. Orion Mach.(Japan)）

11:15 AM - 11:30 AM

Oral Session | Postharvest/Food Technology and Process Engineering
[6-1015-C] Postharvest/Food Technology and Process Engineering (6)
Fri. Sep 6, 2019 10:15 AM - 11:30 AM Room C (3rd room)

[6-1015-C-01] Spatially Resolved Interactance Spectroscopy to Estimate Degree of Red Coloration in Red-fleshed Apple Cultivar 'Kurenai-no-Yume'

*Xujun Ye[1], Sou Takada[1], Shuhuai Zhang[1] (1. Hirosaki University(Japan))

Keywords: Red-fleshed apple, Kurenai-no-Yume, Red coloration, Interactance spectroscopy, Anthocyanin, Non-destructive estimation, Partial least squares regression

Reliable information about degree of red coloration in fruit flesh is essential for grading and sorting of red-fleshed apples. This study used spatially resolved interactance spectroscopy as a new rapid and non-destructive technique to estimate degree of red coloration in the flesh of a red-fleshed apple cultivar 'Kurenai-no-Yume'. A novel measurement device was developed to obtain spatially resolved interactance spectra at eight different light source-detector separations. A UV-Vis-NIR spectrometer connected to the detector fiber was used to obtain interactance spectra ranging from 190~1070 nm for 50 apple fruits. Anthocyanins in apple flesh were first extracted using a solvent extraction technique, and their contents were then quantified based on the absorbance measurements at 530, 620 and 650 nm obtained with a spectrophotometer. Partial least squares (PLS) regression analysis was performed to develop estimation models for anthocyanins content from spatially resolved interactance spectra. Results showed that the PLS models based on interactance spectra obtained at different light source-detector separations achieve different predictive accuracy for anthocyanins estimation. These results suggest that spatially resolved interactance spectroscopy could contribute to identifying an optimal light source-detector distance for implementing the interactance spectroscopy to assess the internal quality of red-fleshed apples. This new approach may be potentially applied to grading and sorting systems for red-fleshed apples in fruit industry.

Spatially Resolved Interactance Spectroscopy to Estimate Degree of Red Coloration in Red-fleshed Apple Cultivar 'Kurenai-no-Yume'

Xujun Ye, Sou Takada, Shuhuai Zhang

Faculty of Agriculture and Life Science, Hirosaki University, Aomori 036-8561, Japan

*Corresponding author: yexujun@hirosaki-u.ac.jp

ABSTRACT

Reliable information about degree of red coloration in fruit flesh is essential for grading and sorting of red-fleshed apples. This study used spatially resolved interactance spectroscopy as a new rapid and non-destructive technique to estimate degree of red coloration in the flesh of a red-fleshed apple cultivar 'Kurenai-no-Yume'. A novel measurement device was developed to obtain spatially resolved interactance spectra at eight different light source-detector separations. A UV-Vis-NIR spectrometer connected to the detector fiber was used to obtain interactance spectra ranging from 190~1070 nm for 50 apple fruits. Anthocyanins in apple flesh were first extracted using a solvent extraction technique, and their contents were then quantified based on the absorbance measurements at 530, 620 and 650 nm obtained with a spectrophotometer. Partial least squares (PLS) regression analysis was performed to develop estimation models for anthocyanins content from spatially resolved interactance spectra. Results showed that the PLS models based on interactance spectra obtained at different light source-detector separations achieve different predictive accuracy for anthocyanins estimation. These results suggest that spatially resolved interactance spectroscopy could contribute to identifying an optimal light source-detector distance for implementing the interactance spectroscopy to assess the internal quality of red-fleshed apples. This new approach may be potentially applied to grading and sorting systems for red-fleshed apples in fruit industry.

Keywords: Red-fleshed apple, Kurenai-no-Yume, Red coloration, Anthocyanin, Interactance spectroscopy, Non-destructive estimation, Partial least squares regression

1. INTRODUCTION

Red-fleshed apples are welcomed by consumers because of their unique flesh colors and additional health benefits offered by more anti-oxidants present in the flesh. 'Kurenai-no-Yume', literally called "crimson dream", is a new red-fleshed apple cultivar bred by Hirosaki University, Japan (Igarashi et al., 2010). Like many other red-fleshed apple varieties, 'Kurenai-no-Yume' suffers from significant difference in flesh red coloration among individual fruits. The degree of red coloration in the flesh cannot be known unless the fruit is cut. Such destructive method can be used to check fruit samples but cannot be applied to all fruits. And checking of only a limited number of samples cannot accurately reflect the degree of red coloration in other fruits even they are from the same batch. Therefore, there is a need to develop an accurate, rapid and non-destructive technique for determining the degree of red coloration for individual fruits. In our previous work, an interactance device was developed to collect interactance spectra for investigating red coloration in apple fruits (Ye et al., 2017). The device obtained interactance spectra with a constant distance between light source and detector fiber. Several models were developed for estimating the degree of red coloration in the flesh, with different levels of accuracy achieved. As a further step of this research, we recently developed a novel measurement device to obtain spatially resolved interactance spectra from apple fruits. The new device could obtain interactance spectra with a detector fiber, whose distance from light source could be adjusted to eight specified distances. In this study, we employed the new device to investigate the feasibility of spatially resolved interactance spectroscopy for estimating the degree of red coloration in the flesh of 'Kurenai-no-Yume' apples.

2. MATERIALS AND METHODS

2.1. Fruit material and sample preparation

'Kurenai-no-Yume', a red-fleshed apple cultivar, was used in this study. The fruit is sweet, mildly tart, rich in anthocyanin, and is delicious either fresh or cooked. The natural red color of flesh remains distinct even after cooking or processing, making it particularly useful for the creation of richly colored apple products (Hirosaki University, 2016). Therefore, it is welcomed by both consumers and manufacturers of apple fruit products.

Trees of this precious cultivar were cultivated in Fujisaki Farm of Hirosaki University. The fruits were harvested in a timely manner and carefully handled during harvest and transport. After screening them to ensure a high degree of fruit size uniformity, a total of 50 fruit samples were selected for the experiment. The flesh of fruit samples showed a large variation in the degree of red coloration (Fig. 1). Further, it was also found that the fruit skin color did not exactly reflect the color of the flesh, suggesting the difficulty to discriminate the flesh color simply based on the skin color of the fruit.

Figure 1. Different degree of red coloration in two 'Kurenai-no-Yume' apple fruits.

2.2. Spatially resolved interactance measurement system

A spatially resolved interactance measurement system was developed for collecting interactance spectra for apple fruits. The system is composed of a halogen light source generator LA-150ue-A (Hayashi Co., Japan), a ring illuminator (Hayashi Co., Japan) integrated with a self-made movable detector fiber, and a mini-spectroscope BLACK-Comet-SR100 (StellarNet Inc., USA) (Fig. 2a). During measurement, the ring illuminator was tightly placed on the fruit surface (Fig. 2b), allowing the halogen light to pass through the fruit skin and enter the flesh, and the amount of light that returned to the detector after scattering in the flesh was measured.

The mini spectroscope covers ultraviolet, visible and near infrared spectroscopic wavelengths from 190-1070 nm. The mini spectroscope is connected to a computer, and the interactance measurements for the sample are recorded when the system is operated by the software SpectraWiz (StellarNet Inc., USA) installed on a PC. Once the data is recorded, the interactance spectra for each measurement can be exported with the software for further analysis.

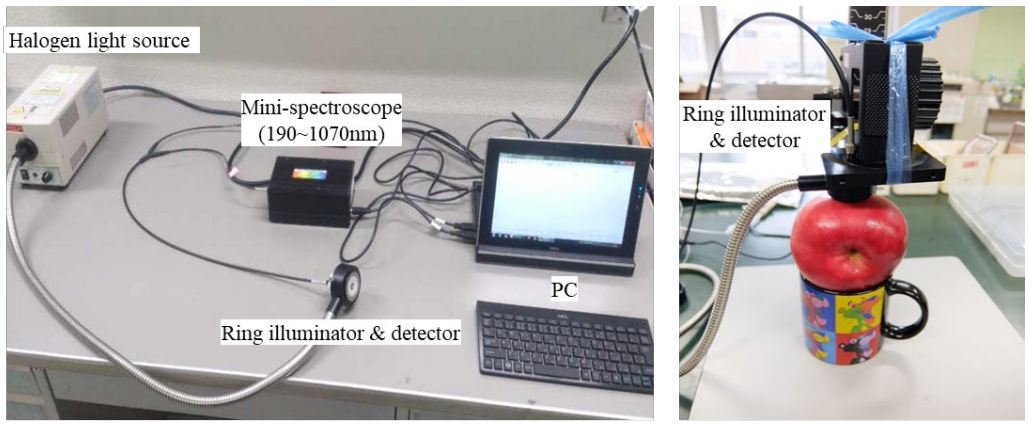

a). Experiment instruments b). Measurement of interactance

Figure 2. Instruments and experimental setup.

The working principle of the above system is described in more detail below. Figure 3a shows the structure of the ring illuminator integrated with the detector. The light from the halogen light source generator enters the ring illuminator through connecting fibers and forms a ring-type light beam (yellow ring) (Fig. 3b). The outer black cover and the inner light shield (black area) block the light that is directly reflected from fruit surface (Fig. 3b). The hole in the center serves as an entrance slit for the light that comes back to the detector after scattering in the flesh and passing back through the fruit skin (Fig. 3ab). In this structure, the light source (ring-type beam) and detector (entrance slit) are positioned parallel to each other, thus light due to specular reflection cannot directly enter the detector. The fibers leading to the source and detector are parallel to each other and in contact with the product (Fig. 2a).
Furthermore, in this structure, the detector is designed to be movable rather than being fixed in the center point of the device. This enables the device to obtain spatially resolved interactance spectra from apple fruits. The new device could obtain interactance spectra with the detector fiber, whose distance from light source could be adjusted to eight specified distances. In Figure 3b, the detector fiber is placed in the center (label 8), which has the farthest distance between the light source and the detector, and the labels 1 to 15 represent different positions of the detector fiber at eight different light source-detector separations.

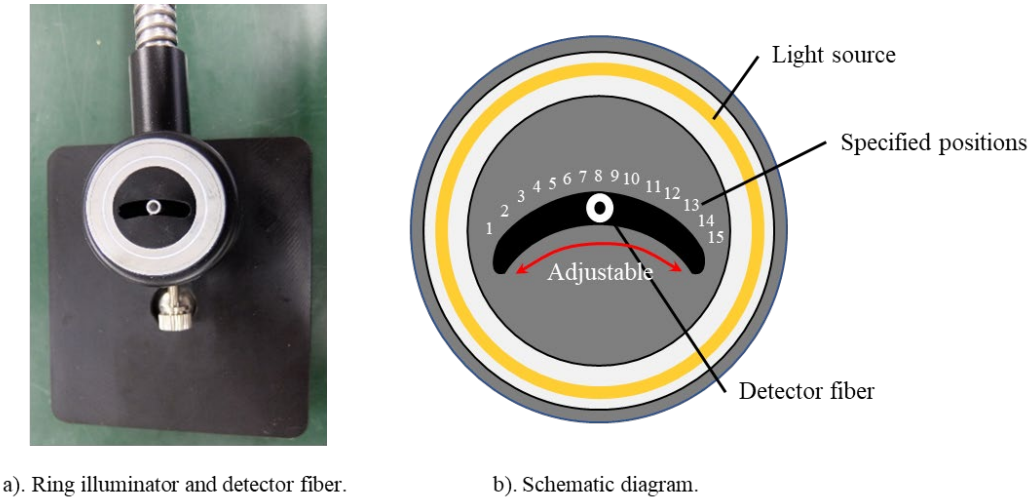

a). Ring illuminator and detector fiber. b). Schematic diagram.

Figure 3. Ring illuminator and detector used to acquire interactance measurements.

2.3. Quantification of anthocyanins contents in apple flesh

In addition to the skin, anthocyanins are also present in large amounts in the flesh of red-fleshed apples. It can be increased up to several hundred-fold in red flesh compared with white flesh (Wang et al., 2014). Therefore, the anthocyanins content can be used as an indicator for the degree of red coloration in the flesh.
After the interactance measurements, the fruit skins of the measured positions were peeled, and the flesh under the peeled skins was cut separately. The cut flesh was weighed and ground to a pulp in a mortar using a pestle. The pulped flesh was subsequently extracted with 10 ml 1% ethyl acetic acid in methanol. The residue was re-extracted multiple times until all pigments were removed. The solvents containing anthocyanins were filtered through a filter paper and then transferred into a separating funnel. After the extractions, the anthocyanins absorbances at 530, 620 and 650 nm were measured with the Spectrophotometer U-2000S (Hitachi Co., Japan), based on which the anthocyanins contents in the flesh were calculated.

2.4. Data analysis and model development

The spatially resolved interactance spectra were used to relate to the anthocyanins content of the apple flesh. The partial least squares (PLS) regression, a standard calibration method for analyzing spectral data (Ramadan et al., 2004), was used to develop the prediction models. We used the R package ‘pls’ for modeling analysis (Mevik and Wehrens, 2007). In the modelling, we employed the leave-one-out

method for cross validation, in which potential models are calculated by excluding only one observation at a time (Kohavi, 1995).

3. RESULTS AND DISCUSSION

3.1Anthocyanins content in apple flesh

The anthocyanins content in the flesh ranged from 0.47 to 42.24 mg/g for the fruit samples, with an average of 9.19 mg/g and standard deviation of 8.95 mg/g, respectively, showing a tremendous difference in the anthocyanins content among fruits, which is responsible for the different degree of red coloration in the flesh among fruits.

3.2. Characteristics of spatially resolved interactance spectra

The spatially resolved interactance spectra were collected by the detector at eight different light source-detector separations. Because no or little interactance was detected in the short wavelength range, the interactances only for the wavelength range from 500 nm to 1070 nm were illustrated (Fig. 4). In Figure 4, except for label 8 of the specific positions (the center of the device), every two of other specific positions, such as labels 1 and 15, labels 2 and 14, etc., have the same distance from the light source, and therefore the averaged interactances of these paired positions were calculated.

The spatially resolved interactance spectra showed significant differences in the signal intensities of interactances among different specific positions, though all specific positions showed a similar pattern along the wavelength range (Fig. 4). The specific position label 8 (the center of the device) showed the lowest interactances, and the interactances increased gradually as the distances of the specific positions from the light source became closer (the spectra shifted upwards). Furthermore, the overall spatially resolved interactances of the fruit sample with a high anthocyanins content were lower than those of the fruit with a lower anthocyanins content, particularly within the 500-660 nm wavelength range. These results suggest that the spatially resolved interactances in these wavelength ranges may provide useful information about the anthocyanins content in apple flesh.

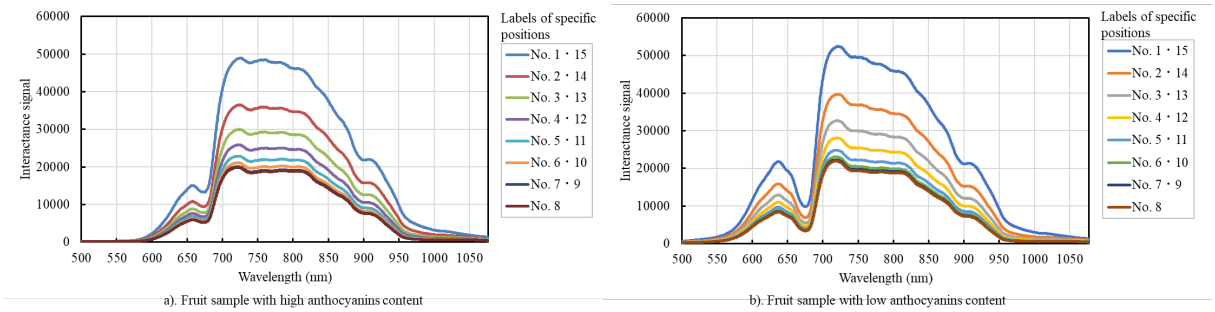

Figure 4. Characteristics of spatially resolved interactance spectra obtained for two fruit samples with high (a) and low (b) anthocyanins contests, respectively.

3.4. PLS models

The averaged interactances of the eight different light source-detector separations were used to develop PLS models. Figure 5 shows the predictive performance of the models for both the calibration and cross validation. It was found that the specific positions of labels 4 and 12 achieved the best predictive performance in both the calibration and cross validation, and the light source-detector separations (labels 1 and 15, 2 and 14, and 3 and 13) with a shorter distance showed a significantly lower predictive accuracy. This might be attributed to the fact that more interactions occur between scattered light and fruit tissues when light passes through a longer distance within the flesh of a fruit, and these interactions enable the collection of interactance spectra with more information about the internal properties of fruits. Nevertheless, the central position (label 8), which has the longest light source-detector separation, demonstrated the lowest prediction accuracy in cross validation, though its performance was better than its neighboring measurement positions. This suggests that when the light source-detector distance exceeds a certain distance limit, the interactance that can be detected might become much less informative because most of the light is absorbed by the flesh and thus cannot reach the detector.

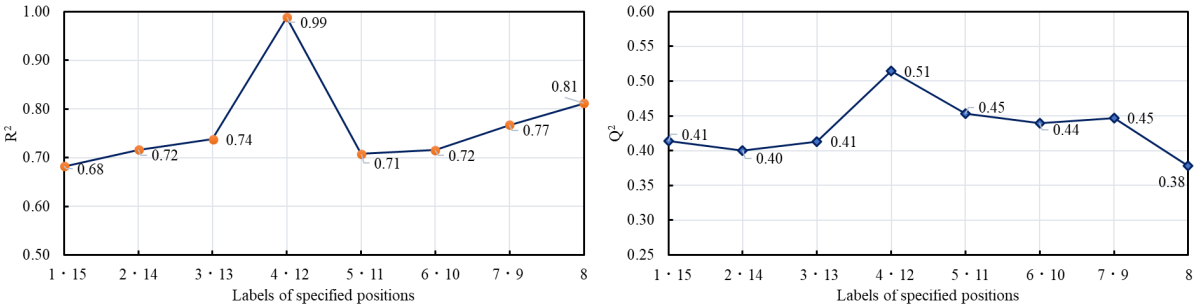

Figure 5. Coefficients of determination for calibration (R^2) and cross validation (Q^2) of PLS regression analysis based on averaged interactances obtained at eight different light source-detector separations.

The PLS model based on the averaged interactances for the optimal light source-detector separations (specific positions label 4 and 12) identified in the previous analysis was developed. Scatter plots of the estimated against the measured anthocyanins contents and the coefficients of determination for the predictions are illustrated in Figure 6. The model achieved a good predictive performance in the calibration (R^2=0.99), and a reasonable predictive accuracy (Q^2=0.51) was also obtained. This result demonstrated the possibility of estimating the anthocyanins content in apple flesh from the interactance spectra obtained with a non-destructive approach.

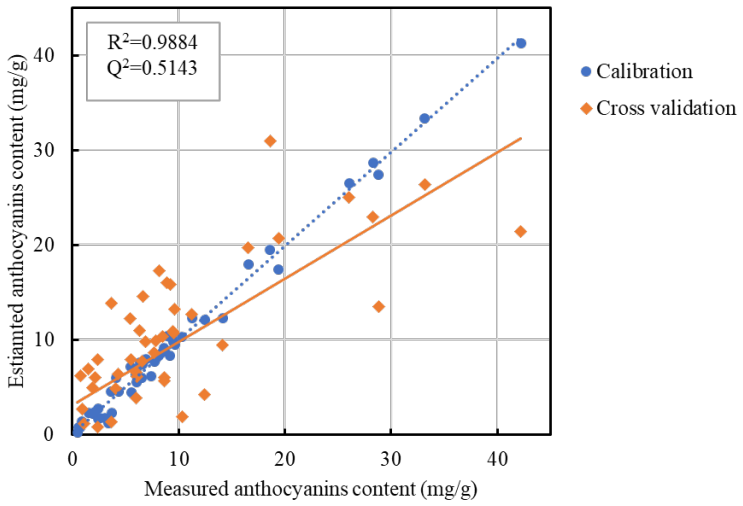

Figure 6. Predictive performance of the PLS model based on averaged interactances obtained at the optimal light source-detector separations (specific positions labels 4 and 12).

4. CONCLUSION

This study investigated the possibility of spatially resolved interactance spectroscopy to estimate the degree of red coloration in the flesh of a red-fleshed apple cultivar 'Kurenai-no-Yume'. A novel measurement device was developed to obtain spatially resolved interactance spectra at eight different light source-detector separations. A UV-Vis-NIR spectrometer (190~1070 nm) connected to the detector fiber was used to collect the spatially resolved interactance spectra for apple fruits. Anthocyanins contents in apple fleshes were quantified using a spectrophotometric method. Partial least squares (PLS) regression analysis was performed to develop predictive models for anthocyanins content from spatially resolved interactance spectra. Results showed that the PLS models based on interactance spectra obtained at different light source-detector separations achieve different predictive accuracy for anthocyanins estimation and increasing the detector's distance from light source tends to

improve the predictive accuracy. This might be attributed to the fact that more interactions occur between scattered light and fruit tissues when incident light passes through a longer distance within the flesh of a fruit, and these interactions enable the collection of interactance spectra with more information about the internal properties of fruits. However, a further increase in the light source-detector distance would lead to reduced predictive accuracy, as the interactances become less informative because most of the light is absorbed by the flesh and thus cannot reach the detector to be captured. This study suggests that spatially resolved interactance spectroscopy could contribute to identifying an optimal light source-detector distance for implementing the interactance spectroscopy to assess the internal quality of red-fleshed apples. This new approach may be potentially applied to grading and sorting systems for red-fleshed apples in fruit industry.

ACKNOWLEDGMENT

The authors acknowledge the financial support received through JSPS KAKENHI Grant Number 17K08028.

REFERENCES

Hirosaki University, 2016. http://nature.cc.hirosaki-u.ac.jp/kurenainoyume/index.html

Igarashi, M., Y. Hatsuyama, K. Matsumoto and Y. Shiozaki 2010. Identification of parents of 'Kurenainoyume', a new cultivar of red-fleshed apple, by DNA markers. *Bull. Fac. Agri. & Life Sci.*, Hirosaki University 13, 7–13

Kohavi, R. 1995. A study of cross-validation and bootstrap for accuracy estimation and model selection. In *Proceedings of the Fourteenth International Joint Conference on Artificial Intelligence*, 2(12), 1137–1143, San Mateo, CA: Morgan Kaufmann.

Mevik, B.H. and R. Wehrens 2007. The pls package: principal component and partial least squares regress in R. *J. Stat. Softw.* 18(2), 1-24.

Ramadan, Z., P. K. Hopke, M. J. Johnson and K. M. Scow 2004. Application of PLS and back-propagation neural networks for the estimation of soil properties. *Chemometr. Intell. Lab. Syst.* 75, 23–30.

Wang, X., C. Li, D. Liang, Y. Zou, P. Li and F. Ma 2015. Phenolic compounds and antioxidant activity in red-fleshed apples. *J. Funct. Foods* 18, 1086–1094

Ye, X., S. Ishioka and S. Zhang 2017. Estimation of the degree of red coloration in flesh of a red-fleshed apple cultivar 'Kurenai no Yume' with a UV-Vis-NIR interactance device. *Postharvest Biology and Technology*, 124, 128-136.

Oral Session | Postharvest/Food Technology and Process Engineering
[6-1015-C] Postharvest/Food Technology and Process Engineering (6)
Fri. Sep 6, 2019 10:15 AM - 11:30 AM Room C (3rd room)

[6-1015-C-02] Use of hyperspectral imaging to separate cultivars and evaluate the internal quality of nectarines

Sandra Munera[1], Prieto Andres[1], Nuria Aleixos[2], Sergio Cubero[1], *Jose Blasco[1] (1. Centro de Agroingeniería. Instituto Valenciano de Investigaciones Agrarias (IVIA). Ctra. Moncada-Náquera Km 4.5, 46113, Moncada, Valencia(Spain), 2. Departamento de Ingeniería Gráfica. Universitat Politècnica de València. Camino de Vera, s/n, 46022 Valencia(Spain))

Keywords: Stone fruit, Hyperspectral transmittance imaging, Ripeness monitoring, Cultivar discrimination, Internal quality, Computer vision

Visible–near-infrared hyperspectral imaging (450-1040 nm) was studied in reflectance and transmittance modes to assess the internal physicochemical properties and sensory perception of 'Big Top' and 'Magique' nectarines (*Prunus persica* L. Batsch var. *nucipersica*) (yellow and white-flesh cultivar, respectively) during ripening. These properties were successfully correlated to the Ripening Index (RPI) and the Internal Quality Index (IQI). During ripeness under controlled conditions, hyperspectral images of the intact fruits were acquired and their physicochemical properties (flesh firmness, total soluble solids, titratable acidity and flesh colour) were analysed. Moreover, a model to discriminate between both cultivars were developed. IQI and RPI were correlated to the hyperspectral images by using Partial Least Square (PLS) regression with proper variables selection. Optimal results were obtained with R^2 (and RPD) values of 0.89 (2.7), 0.90 (3.1), 0.90 (2.8) and 0.88 (2.7) for RPI and IQI in 'Big Top' and 'Magique' nectarines, respectively.

In addition, the emergence of new cultivars in the market with similar appearance but different sensory properties can cause confusion among the consumers, being necessary the development of new tools capable of discriminating these cultivars in an automated and non-destructive way. PLS-DA was used to obtain the best classification model to distinguish intact fruits of both cultivars using individual pixel spectrum and mean spectrum of each fruit, and then projecting the model onto the complete surface of fruits in a validation or prediction set. The results indicated that mean spectrum approach was the most accurate, 84.4 % vs. 94.4 %. Moreover, a comprehensive wavelength selection was performed, reducing the dimensionality of the hyperspectral images using the regression coefficients of the mean spectrum PLS-DA model, obtaining an accuracy of 96.3 % by using 14 optimal wavelengths.

A PLS model of IQI prediction was used to transfer the calibrated results to each pixel of the image and to visualise the evolution of ripeness on the surface of the fruits, and also to represent the probability of whether any pixels belongs to one or another cultivar.

Finally, the internal quality of the nectarines was inspected using hyperspectral transmittance imaging during their ripening under controlled conditions. The detection of split pit disorder and classification according to an established firmness threshold were performed using PLS-DA. The prediction of the IQI related to ripeness was performed using PLS-R. The most important variables were selected using interval-PLS. As a result, an accuracy of 94.7 % was obtained in the detection of fruits with split pit of the 'Big Top' cultivar. Accuracies of 95.7 % and 94.6 % were achieved in the classification of the 'Big Top' and 'Magique' cultivars, respectively, according to the firmness threshold. The internal quality was predicted through the IQI with R^2 values of 0.88 and 0.86 for the two cultivars. The results obtained indicate the great potential of hyperspectral

Use of hyperspectral imaging to separate cultivars and evaluate the internal quality of nectarines

Sandra Munera[a], Andres Prieto[a], Nuria Aleixos[b], Sergio Cubero[a], José Blasco[a*]

a) Centro de Agroingeniería, Instituto Valenciano de Investigaciones Agrarias (IVIA). Carretera CV-315, Km 10.7, 46113 Moncada, Spain. *Corresponding author: blasco_josiva@gva.es Tel.: +34 961465315

b) Departamento de Ingeniería Gráfica. Universitat Politècnica de València. Camino de Vera, s/n, 46022 Valencia, Spain. naleixos@dig.upv.es

Visible–near-infrared hyperspectral imaging (450-1040 nm) was studied in reflectance and transmittance modes to assess the internal physicochemical properties and sensory perception of 'Big Top' and 'Magique' nectarines (*Prunus persica* L. Batsch var. *nucipersica*) (yellow and white-flesh cultivar, respectively) during ripening. These properties were successfully correlated to the Ripening Index (RPI) and the Internal Quality Index (IQI). During ripeness under controlled conditions, hyperspectral images of the intact fruits were acquired and their physicochemical properties (flesh firmness, total soluble solids, titratable acidity and flesh colour) were analysed. Moreover, a model to discriminate between both cultivars were developed. IQI and RPI were correlated to the hyperspectral images by using Partial Least Square (PLS) regression with proper variables selection. Optimal results were obtained with R^2 (and RPD) values of 0.89 (2.7), 0.90 (3.1), 0.90 (2.8) and 0.88 (2.7) for RPI and IQI in 'Big Top' and 'Magique' nectarines, respectively.

In addition, the emergence of new cultivars in the market with similar appearance but different sensory properties can cause confusion among the consumers, being necessary the development of new tools capable of discriminating these cultivars in an automated and non-destructive way. PLS-DA was used to obtain the best classification model to distinguish intact fruits of both cultivars using individual pixel spectrum and mean spectrum of each fruit, and then

projecting the model onto the complete surface of fruits in a validation or prediction set. The results indicated that mean spectrum approach was the most accurate, 84.4 % vs. 94.4 %. Moreover, a comprehensive wavelength selection was performed, reducing the dimensionality of the hyperspectral images using the regression coefficients of the mean spectrum PLS-DA model, obtaining an accuracy of 96.3 % by using 14 optimal wavelengths.

A PLS model of IQI prediction was used to transfer the calibrated results to each pixel of the image and to visualise the evolution of ripeness on the surface of the fruits, and also to represent the probability of whether any pixels belongs to one or another cultivar.

Finally, the internal quality of the nectarines was inspected using hyperspectral transmittance imaging during their ripening under controlled conditions. The detection of split pit disorder and classification according to an established firmness threshold were performed using PLS-DA. The prediction of the IQI related to ripeness was performed using PLS-R. The most important variables were selected using interval-PLS. As a result, an accuracy of 94.7 % was obtained in the detection of fruits with split pit of the 'Big Top' cultivar. Accuracies of 95.7 % and 94.6 % were achieved in the classification of the 'Big Top' and 'Magique' cultivars, respectively, according to the firmness threshold. The internal quality was predicted through the IQI with R^2 values of 0.88 and 0.86 for the two cultivars. The results obtained indicate the great potential of hyperspectral imaging as a tool of non-destructive monitoring of the quality of nectarines.

Oral Session | Postharvest/Food Technology and Process Engineering
[6-1015-C] Postharvest/Food Technology and Process Engineering (6)
Fri. Sep 6, 2019 10:15 AM - 11:30 AM Room C (3rd room)

[6-1015-C-03] Evaluating the Performance of Unmanned Crop Sensing Robot for Rice

*Dhirendranath Singh[1], Shigeru Ichiura[1], Mitsuhiko Katahira[2,1] (1. United Graduate School of Agriculture , Iwate University(Japan), 2. Faculty of Agriculture, Yamagata University(Japan))

Keywords: Crop Sensing, Unmanned Ground Vehicle (UGV), Precision Agriculture, Rice

Precision Agriculture has emerged as a new scientific field that seeks to drive agricultural productivity while minimizing its environmental impacts. As the demand for food increases, farmers are in search of technology that would allow them cultivate more land with less labour at the same time increasing their productivity. In rice cultivation, this has led to the adoption of technologies such as Unmanned aerial vehicles (UAV) for crop monitoring. While this has increased precision from traditional satellite images, it still has the limitation of being restricted to capturing images of the crop canopy. Unmanned Ground Vehicles (UGV) on the other hand has the potential to capture a wider range of data with pin point accuracy. This paper reports on the work done thus far in evaluating the performance of a field robot developed by the World Wide Food Platform, Japan for rice crop sensing. The study was conducted in 3 rice fields at the Yamagata University' s Farm in Takasaka, Tsurouka, Japan and a Farmers' Field in Mikawa, Yamagata, Japan. The cultivation system in the fields were transplanting, hilldrop and broadcasting at Takasaka, while in Mikawa drill seeding was done. The robot is equipped with sensors for temperature, humidity, sunlight, wind speed, soil temperature, water level and temperature and cameras (Sony FDR-X3000) for image capture. RTK GPS was used for location logging with an accuracy of 5 cm. Data captured were mapped into QGIS 3.4 for visualization an analysis of growth parameters every two weeks after germination, with observations made on the robots' maneuverability in the various field conditions. Plant height, leaf and tiller number, and SPAD values were collected manually in each field to compare for image data. It was found that the robot was able to maneuver in different field conditions without major issue, utilizing the reverse function instead of turning full circle appears to be the most efficient method for turning while causing minimal damage to young seedlings. The weight distribution will have to be considered to obtain optimum performance in deep fields. Data collected from the array of sensors and cameras provides location specific information throughout the field and can be used to guide farmers in precision management.

Evaluating The Performance of Unmanned Crop Sensing Robot for Rice

Dhirendranath SINGH[1], Shigeru ICHIURA[2], Mitsuhiko KATAHIRA[3],

[1,2]Department of Agricultural and Environmental Engineering, Biotic Environmental Science, The United Graduate School of Agriculture Sciences, Iwate University (UGAS)
[2]Department of Food, Life and Environment, Faculty of Agriculture, Yamagata University, 1-23, Wakabamachi, Tsuruoka, Yamagata, 998-8555, Japan.

*Corresponding author: dinosingh19@gmail.com

ABSTRACT

Precision Agriculture has emerged as a new scientific field that seeks to drive agricultural productivity while minimizing its environmental impacts. As the demand for food increases, farmers are in search of technology that would allow them cultivate more land with less labour at the same time increasing their productivity. In rice cultivation, this has led to the adoption of technologies such as Unmanned aerial vehicles (UAV) for crop monitoring. While this has increased precision from traditional satellite images, it still has the limitation of being restricted to capturing images of the crop canopy. Unmanned Ground Vehicles (UGV) on the other hand has the potential to capture a wider range of data with pin point accuracy. This paper reports on the work done thus far in evaluating the performance of a field robot developed by the World Wide Food Platform, Japan for rice crop sensing. The study was conducted in 3 rice fields at the Yamagata University's Farm in Takasaka, Tsurouka, Japan and a Farmers' Field in Mikawa, Yamagata, Japan. The cultivation system in the fields were transplanting, hilldrop and broadcasting at Takasaka, while in Mikawa drill seeding was done. The robot is equipped with sensors for temperature, humidity, sunlight, wind speed, soil temperature, water level and temperature and cameras (Sony FDR-X3000) for image capture. RTK GPS was used for location logging with an accuracy of 5 cm. Data captured were mapped into QGIS 3.4 for visualization an analysis of growth parameters every two weeks after germination, with observations made on the robots' maneuverability in the various field conditions. Plant height, leaf and tiller number, and SPAD values were collected manually in each field to compare for image data. It was found that the robot was able to maneuver in different field conditions without major issue, utilizing the reverse function instead of turning full circle appears to be the most efficient method for turning while causing minimal damage to young seedlings. The weight distribution will have to be considered to obtain optimum performance in deep fields. Data collected from the array of sensors and cameras provides location specific information throughout the field and can be used to guide farmers in precision management.

Keywords: Crop Sensing, Unmanned Ground Vehicle (UGV), Precision Agriculture, Rice

1. INTRODUCTION

Agriculture plays a critical role in feeding the 7.6 billion people in the world. With the available labour for agriculture declining as demand for food increases, farmers and researchers are exploring the application of technologies that will allow for more land to be cultivated with a reduced labour force while at the same time maintaining productivity. In rice cultivation, this has led to the adoption of technologies such as Unmanned aerial vehicles (UAV) for crop monitoring. While this has increased precision from traditional satellite images, it still has the limitation of being restricted to capturing images of the crop canopy. Unmanned Ground Vehicles (UGV) on the other hand has the potential to capture a wider range of data with pin point accuracy. Work on unmanned vehicles with respect to rice has mainly been focused on adapting conventional farm machinery to execute task without human intervention. Commercially available

tractors can be modified into autonomous vehicles by adding the electronics and communication devices necessary for autonomous operation in agricultural fields (Aravind et al. 2017). TAKAI et al. (2010) modified a crawler-type tractor and evaluated its accuracy for autonomous navigation using RTK-GPS and IMU navigation sensors while Tamaki et al. (2013) explored a robot system for tillage, transplanting and harvesting rice by adapting conventional machinery. They showed it was possible for one operator to operate more than one machine thereby reducing the time and labour necessary for a specific task. Because of their size and potential injury to crop, the adapted farm machinery is not suitable for crop sensing, as a result, this aspect of crop production is being done by UAVs, stationary infield sensors and human labour. Compared to UAVs and stationary sensors, a ground robot designed to traverse the rice field with minimal damage to crop offers more detail crop sensing information with greater accuracy. In this study, we evaluate the performance of a field robot developed by the World Wide Food Platform, Japan for rice crop sensing.

2. MATERIALS AND METHODS

2.1 Location

The study is being conducted in three experiment plots for rice at the Yamagata University's Farm in Takasaka, Tsuruoka, Japan and one farmer field in Mikawa, Yamagata, Japan. The cultivation system in the fields were transplanting, hilldrop and broadcasting at Takasaka while drill seeding was done at Mikawa. Field dimensions are 30m x 8m for the transplant and hill drop fields while the drill seeding and broadcast fields were 100m x 30m.

2.2 Equipment

2.2.1 Field Robot outline

The field robot used in this study was developed by the World Wide Food Platform, Japan which is a consortium of Tech companies, Universities and Farmers' Organizations. It is 140 cm in length, 120cm width and 145 cm height. Approximate weight is 180 kg. Two 12 volt batteries supply power to 4 brushless electric motors (200W, 3000r/min Orientalmotor, Model BLVM620KM-GFS, Japan) that rotate each the four wheels. The wheel diameter is 65cm and is of similar type used on rice transplanting machines. The drive controller is Ardupilot pixhawk 2 while the operation of the robot is by remote control.

Figure 1. Front & Side view of crop sensing robot and remote controller

2.2.2 Sensor Box

A sensor box containing sensors for Temperature and Humidity (SHT31 module), sunshine (Sanko PV Array Pryanometer PVSS-01), Airspeed (Powerday Airspeed sensor), water temperature (Thermistor 103AT-11), water level (Distance sensor MB1242) is mounted unto the robot with RTK GPS attached. Data recorded by sensorbox is stored on micro SD card.

2.2.3 RTK GPS

Here+ RTK GPS rover and base station was used with Mission Planner for GPS logging. Base station data was recorded for 5 days to obtain an accuracy of 5cm for each plot.

2.2.4 Camera

Two Sony FDR-X3000 action cameras were used for image capture. Images were captured in HD (1920 x 1080 pixels). Three orientations were explored with mounting cameras on the robot with the aim of acquiring suitable images. In the first instance Fig.2 (a) the camera was mounted directly on the robot facing downward at an approximate angle of 45 degrees. In the second orientation, camera mounts were used to extend the cameras 25cm from the robot with an approximate angle of 45 degrees, while the third orientation consisted extending the cameras 90 cm from the robot at an angle of 90 degrees. The images were captured from a height of 110 cm with the distance between the two cameras 100 cm. Considerations for suitable images were those that were clear, presented a full picture of the plants without any obstruction or unnecessary scenery that would necessitate further processing or transformation before image analysis can be executed. As such, the camera orientation was adjusted as described above until the desired results were achieved.

(a)  (b)  (c) 

Figure 2. Camera orientation on Robot

2.3 Data collection

2.3.1 Data Collection with Robot

Data collection with the robot commenced at the end of May 2019 when plants were at the 5 leaf stage. In addition to image and sensing data, observations were made on robot maneuverability in rice fields, damage to plants, operation time and speed. Figure 3 shows the base station set up for data collection. The RTK antenna is placed at the same location where base station data was captured for 5 days to obtain an accuracy level of 5cm. It is connected to the RTK base station which is connected to the Note PC via USB. The link between the PC and robot is made via a UDP WiFi connection with pixhwak in the sensor box through the Misson Planner Software.

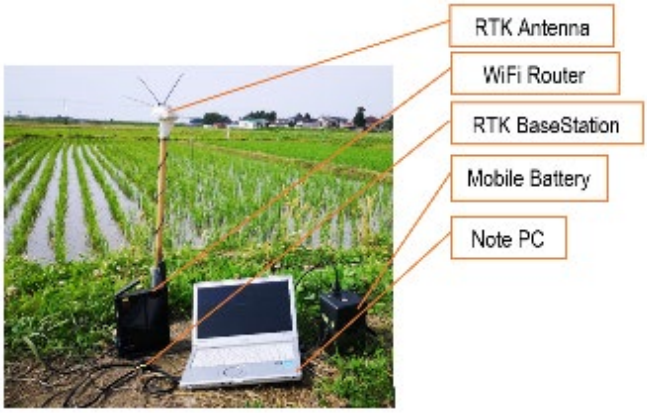

Figure 3. Base Station set up during data Collection

2.3.2 Manual Data collection

Growth data was collected manually either directly after data collection with robot or within 48hours depending on weather conditions. Three test plots were randomly selected in each field and demarcated. SPAD, plant height, number of tillers, and leaf number surveyed at two week intervals after germination. SPAD was measured using SPAD-502 Plus (Konica Minolta, Japan).

2.4 Data Processing

Data recorded by sensor box were converted from .bin to .log files in using Mission Planner (Version 1.3 by Michael Osborne). A user defined Python (3.6) script was then use to parse data from the .log files and write to .csv file. The .csv file was then imported into QGIS (version 3.4 LTR) and vector layers created for areas of interest; Altitude, Temperature, Humidity, Air Speed, Sunshine. Images captured were imported into QGIS via the Import Photos plugin to provide an image for each point captured.

3. RESULTS AND DISCUSSION

3.1 Robot

3.1.1 Maneuverability in Rice Fields.

Observations were made on the robot's ability to maneuver in the rice fields. The robot covers four rows in one pass with wheels travelling between rows. It is able to effect turns by stopping motors on one side while the other side continues to move (like pivot system). The smallest turning diameter on dry surface was 160 cm, however in effecting this turn there is sliding /dragging of the unmoving wheels of approximately 30 cm. Attempting such turn in flooded field conditions resulted in longer sliding distance and dislodged or damaged seedlings. In some cases, the wheel also locked and a reboot was required to free the wheels.

Executing a gentler turn requires a turning diameter of approximately 250 cm. In this turn all wheels move turning slightly until the turn is complete. This method reduces the sliding/dragging of wheel and results in very few damaged or dislodge seedlings. Executing turns in this manner however requires more space and also will leave gaps in the field at turning points with respect to data collection (Fig. 4 a) before the robot can enter the set of rows.

The best turning method devised thus far involves utilizing the robot's ability to reverse freely. In this method, instead of turning 360 degrees, just prior to reaching the end of the row, the robot makes a slight turn to exit the row and then reverse into the new set of rows (Fig.4b), only when it reaches the end of those rows, it turns slightly to enter the new set of rows by going forward. Operation using this 'switchback' method reduces the amount of degree the robot has to turn resulting in minimal damage or dislodgement of seedlings. It also makes it easy to enter the next set or rows without missing any data. Figure 4(c, d) shows the actual path travelled by the robot using the two methods.

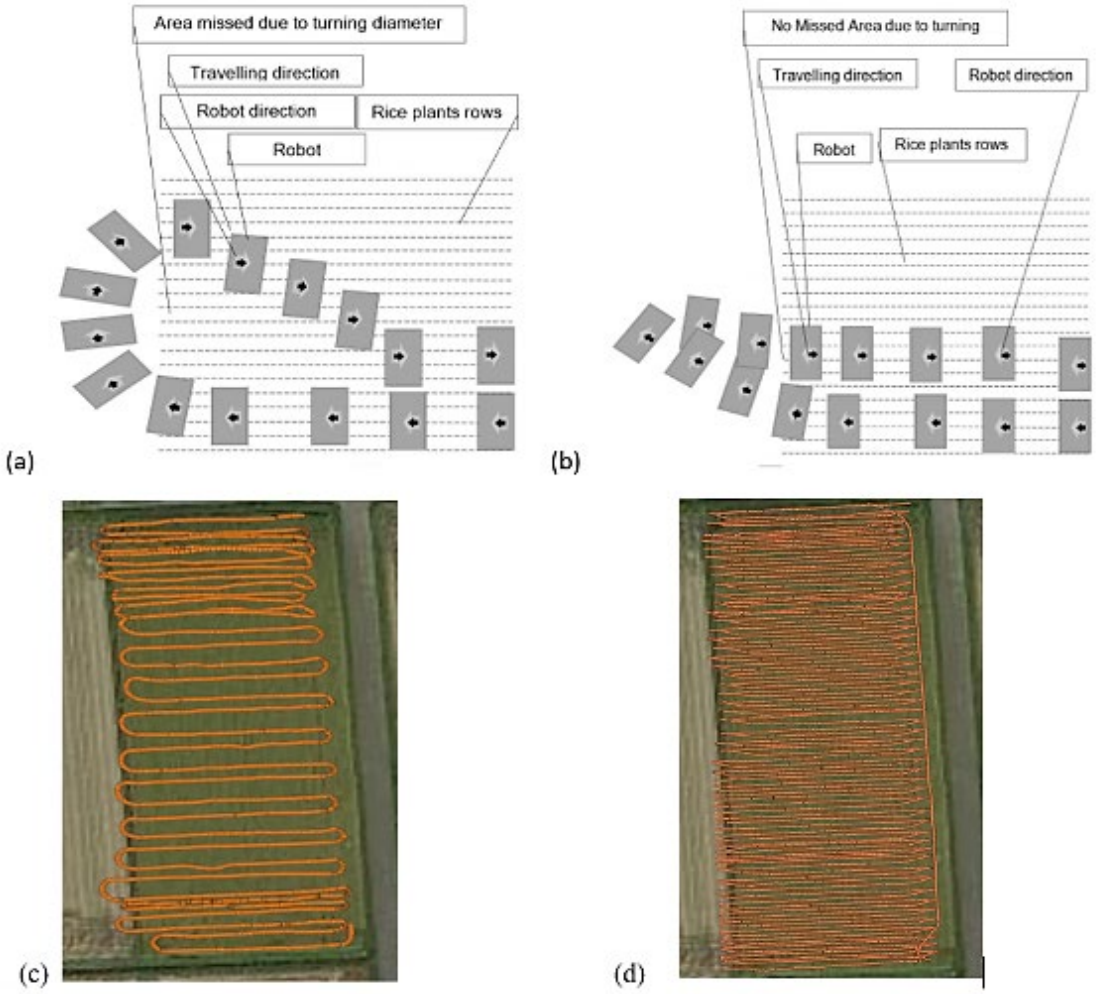

Figure 4. Turning methods (a,b) and actual path travelled by robot using each method (c,d)

3.1.2 Speed

Speed of robot was recorded by flight controller in meters per second (m/s) which ranged from 0.1 m/s at its lowest speed to 0.6 m/s with 0.3-0.4 m/s being the most common /steady speed. Time require to survey 0.3 ha (30m x100m) field ranges between 2.5-3 hours depending on the amount of overlap (rows) is required.

3.1.3 Field Condition

The robot was able to traverse various rice fields in flooded condition without any major issue. The wheel reduces its ability of getting stuck. It was able to traverse in a field where the mud was approximately 35cm in depth, however very wide turns had to be taken in this situation. Attempts to make small or sharp turns resulted in churning of mud and locking of wheels. It was able to operate freely when going straight and turn by making wide gentle turns. One area that may require further consideration is the weight distribution as there is a tendency to tilt forward or backward especially in deep fields when torque is applied (Fig.5).

Figure 5. Robot in Deep Field Condition

In fields in which the water was drained and the mud had stiffened to some extent, it was observed that the robot tilted heavily rearward while the front wheels tend to lift off the ground when torque was applied with the threat of tilting over (Fig. 6).

Figure 6. Robot in drained field

This situation arose due to the lack of water which cause the mud loosened by the front wheels to stick to the back wheel adding more weight and friction with the soil thus requiring more torque for it to move. The front wheels are not affected by such impediments as such, when the power is applied it surges forward while the rear is being held back resulting the front wheels going aerial. It is suspected that this situation may be remedied by extending the wheel based of the robot and adding scrapers to the wheels to remove excess mud that may become stuck on it while operating in drier fields.

3.2 Camera Orientation

Images captured on the 30th May, 10th June and 2nd July 2019 in Mikawa field from the three camera orientation is shown in Fig3. The first camera orientation (Fig.7a) captures the surrounding scenery in the image in addition to the plants, this is reduced to some extent in images captured in camera orientation

two (Fig.7b) however the angle obscures details in parts of the image. Adjusting these mounting methods to orient the camera at 90 degrees results in images that include the wheel and parts of the robot. Camera orientation three (Fig.7c) that extends from the robot and captures the images from directly above appears to be the most suitable for image capture as no unnecessary information is contained in the images and details are not obscured in any part of the image.

(a)  (b)  (c) 

Figure 7. Images captured by different camera orientations

3.3 Data

The data collected by the robot are field gives information of the field environment, record measurements and captures images. Data collected for field environment includes temperature, humidity, sunshine and airspeed. While these conditions may vary depending on climatic conditions, time of day data is collected as well as over the total time taken to collect the data, as more data is collected patterns may emerge that point to specific location based issues in the field irrespective of the factors mentioned above. In Figure 7 data collected by the robot on the 2nd of July 2019 is shown as QGIS layers for temperature, humidity, sunshine and airspeed for the Mikawa field. The temperature layer (Fig.7a) shows how temperature varies across the field with the highest temperature being observed around the center and reduces as it gets to the lower end. While this may be due to the time data collection started and conditions changing in the duration it take for the robot to reach the lower end of the field. If a similar pattern persist as more data is collected at different time and prevailing weather conditions, it give some insight as to what is happening in the field with respect to temperature. Optimal Temperature for rice growth is considered to be 22-28°C, as such any increase in mean temperature or episodes of high temperature during sensitive stages of the crop may adversely affect the growth and yield of the crop (Krishnan, Ramakrishnan, Reddy, & Reddy, 2011).

(a) 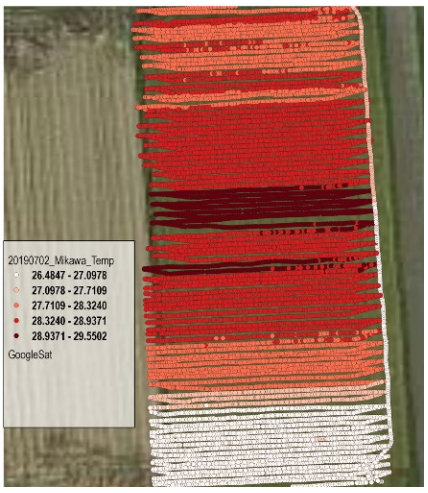

(b) 

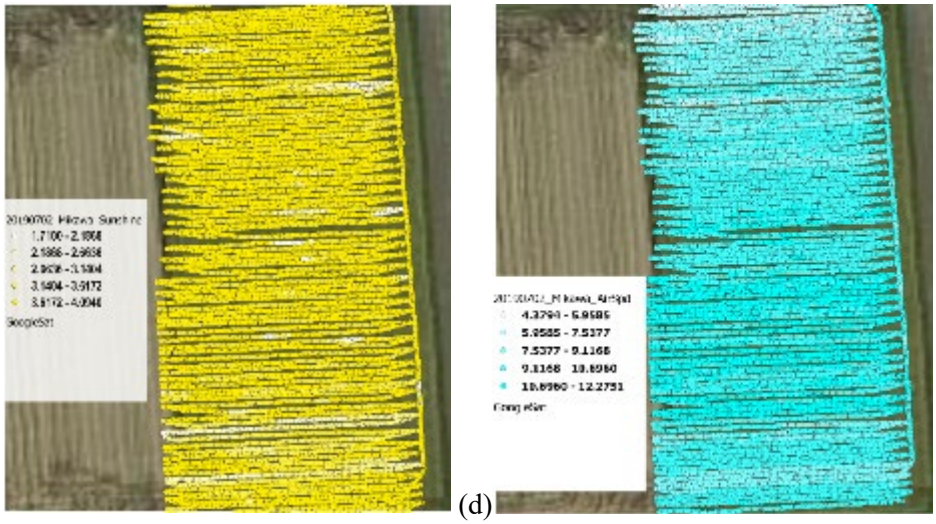

Figure 8. Data collected by Robot in Mikawa field, 2019/07/02: (a) Temperature, (b) Humidity, (c) Sunshine, (d) Airspeed.

The mean relative humidity during rice cultivation is generally negatively associated with solar radiation. Krishnan et al., (2011) discusses works by Morokuma and Yasuda,(2004), Nishiyama and Satake (1981) and Matsui et al., (1997) that reports on increases in spikelet sterility with increases humidity at high air temperatures. They further suggest that the effects of temperature on rice may be intermingled with those of relative humidity and solar radiation. Given the various effects these environmental factors may have on the crop, being able to monitor their distribution over the field may provide insights on how to better manage the field.

The altitude recorded by pixhawk indicates the robot's altitude in meters (m) from sea level. From the plot of this layer in QGIS, it is possible to infer how level the field is, and identify areas that appear too high or low. Figure 9 shows the plot of Altitude data collected at Mikawa on the 2nd of June 2018 where varying altitude is recorded over the field indicating that specific parts of the field is higher and lower than others.

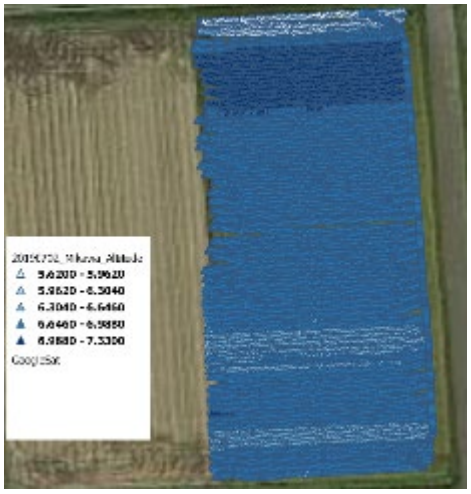

Figure 9. Plot of Altitude recorded in Mikawa Field on 2nd July, 2019

Image Data

Two Sony FDR-X3000 action cameras were used for image capture. Time lapse images at one image per second were captured in HD (1920 x 1080 pixels). The images were geotagged and imported into QGIS to provide an image for each point in the field. These images provide a clear picture at each point of the field with a level of detail not possible with UAVs without the use of expensive high specification cameras. From the images it was possible to identify the presence of weeds in the field as seed in Figure 10 which shows a sample image captured by the cameras. Future work will involve building deep learning AI to detect weeds, insect pests and disease in the field and generate location map for precision management. Attempts will also be made to extract growth data from images by analysis plant canopy for height, tiller and greenness.

Figure 10. Sample Image from Mikawa Field on 2nd July, 2019

4. CONCLUSION

The paper reports on the initial results obtained while evaluating the performance of crop sensing robot for rice. It was found that the robot was able to maneuver in different field conditions without major issues and utilizing the reverse function instead of turning full circle appears to be the most efficient method for turning while causing minimal damage to young seedlings. The weight distribution will have to be considered to obtain optimum performance in deep fields. Data collected from the array of sensors and cameras provides location specific information throughout the field and can be used to guide farmers in precision management. Given that this is the first season of testing, various applications and analysis will be explored with the data gathered to allow for refining and optimizing of the methodologies for next season.

ACKNOWLEDGMENT

Gratitude is expressed to the Worldwide Japan Food Platform (W-JFoP) Consortium for providing the necessary resources and technical support for the execution of this research.

REFERENCES

Aravind, Krishnaswamy R.; Raja, Purushothaman; Pérez-Ruiz, Manuel (2017): Task-based agricultural mobile robots in arable farming: A review. In *Span J Agric Res* 15 (1), e02R01. DOI: 10.5424/sjar/2017151-9573.

Krishnan, P., Ramakrishnan, B., Reddy, K. R., & Reddy, V. R. (2011). *High-Temperature Effects on Rice Growth, Yield, and Grain Quality*. *Advances in Agronomy* (1st ed., Vol. 111). Elsevier Inc. https://doi.org/10.1016/B978-0-12-387689-8.00004-7

TAKAI, Ryosuke; BARAWID, Oscar; ISHII, Kazunobu; NOGUCHI, Noboru (2010): Development of Crawler-Type Robot Tractor based on GPS and IMU. In *IFAC Proceedings Volumes* 43 (26), pp. 151–156. DOI: 10.3182/20101206-3-JP-3009.00026.

Tamaki, K.; Nagasaka, Y.; Nishiwaki, K.; Saito, M.; Kikuchi, Y.; Motobayashi, K. (2013): A Robot System for Paddy Field Farming in Japan. In *IFAC Proceedings Volumes* 46 (18), pp. 143–147. DOI: 10.3182/20130828-2-SF-3019.00013.

Oral Session | Postharvest/Food Technology and Process Engineering
[6-1015-C] Postharvest/Food Technology and Process Engineering (6)
Fri. Sep 6, 2019 10:15 AM - 11:30 AM Room C (3rd room)

[6-1015-C-04] Application of Non-destructive Determination of Rice Amylose Content at Grain Elevators

*Edenio Olivares Diaz[1], Shuso Kawamura[1], Miki Matsuo[1], Toru Nagata[2], Shigenobu Koseki[1] (1. Hokkaido University(Japan), 2. Hokkaido Research Organization Central Agricultural Experiment Station(Japan))

Keywords: Oryza sativa L., Amylose content, Near-infrared spectroscopy, Chemometric analyses, Quality, Practical application

Rice (*Oryza sativa* L.) is the most important staple food for people in a large part of the world. Starch, moisture, and protein are the major constituents comprising the rice endosperm. However, amylose content (AC), which is the percentage of amylose relative to total starch in the rice kernel, contributes to the texture and quality of cooked rice. Iodine-binding, also known as iodine colorimetry or amylose-iodine, is the only validated and most commonly used method for determining AC. But it is labor-intensive, time-consuming, chemical-dependent, and vulnerable to random error. Therefore, it is unsuitable for laboratory and/or industrial uses where large volumes of samples need to be processed. To overcome this shortcoming, near-infrared (NIR) spectroscopy in combination with chemometric techniques represents an alternative, validated method for assessing rice AC. In this study, we developed an accurate model for the non-destructive determination of AC at grain elevators. A dual-step calibration model was developed using data from 936 samples of 10 varieties of rice produced between 2008 and 2018 in various regions of Hokkaido, Japan. The collected rough rice samples were dried to approximately 15% w.b. of moisture content. Next, each dried sample was hulled to obtain brown rice. Finally, each brown rice sample was milled to 90.5 ± 0.2% of milling degree. Milled rice AC reference values (AC_{ref}), transmittance NIR spectra, and physicochemical properties were combined to develop the dual-step calibration model. The raw NIR transmittance spectra was preprocessed by applying a 2^{nd} order Savitzky-Golay derivative with a 2^{nd} polynomial order. Later, AC_{ref} values, transformed NIR spectra, and physicochemical properties were analyzed by partial least squares regression (PLS) and multiple linear regression (MLR) to develop an accurate dual-step calibration model. Our dual-step calibration model described low and ordinary amylose varieties models, which were developed individually. Both the low and ordinary amylose varieties models were calibrated using 2008-2017 production year samples (n = 903) and validated by distinct 2018 production year samples (n = 33), which were collected at a rice grain elevator. Next, the dual-step calibration model was created by merging the validation results of the low and ordinary amylose varieties models. Results indicated that AC_{ref} values were determined with high accuracy based on the low average standard error of the laboratory method (SEL) = 0.17% among varieties and production years. Also, the regression coefficients of each wavelength related to AC_{ref} for the optimal PLS factor indicated that the wavelength at 916 nm reported the highest spectral variation and thus correlated the most to AC. Moreover, validation statistics such as standard error of prediction (SEP) = 0.33% and ratio of performance deviation (RPD) = 5.09 indicated the high robustness and accuracy of the dual-step model, enabling more precise, accurate, and efficient rice quality screening at Japanese grain elevators.

Application of Non-destructive Determination of Rice Amylose Content at Grain Elevators

Edenio Olivares Diaz[1*], Shuso Kawamura[1], Miki Matsuo[1], Toru Nagata[2], Shigenobu Koseki[1]

[1] Graduate School of Agricultural Science, Hokkaido University, Japan
[2]Hokkaido Research Organization Central Agricultural Experiment Station, Japan

*Corresponding author: edeniood@frontier.hokudai.ac.jp

ABSTRACT

Rice (*Oryza sativa* L.) is the most important staple food for people in a large part of the world. Starch, moisture, and protein are the major constituents comprising the rice endosperm. However, amylose content (AC), which is the percentage of amylose relative to total starch in the rice kernel, contributes to the texture and quality of cooked rice. Iodine-binding, also known as iodine colorimetry or amylose-iodine, is the only validated and most commonly used method for determining AC. But it is labor-intensive, time-consuming, chemical-dependent, and vulnerable to random error. Therefore, it is unsuitable for laboratory and/or industrial uses where large volumes of samples need to be processed. To overcome this shortcoming, near-infrared (NIR) spectroscopy in combination with chemometric techniques represents an alternative, validated method for assessing rice AC. In this study, we developed an accurate model for the non-destructive determination of AC at grain elevators. A dual-step calibration model was developed using data from 936 samples of 10 varieties of rice produced between 2008 and 2018 in various regions of Hokkaido, Japan. The collected rough rice samples were dried to approximately 15% w.b. of moisture content. Next, each dried sample was hulled to obtain brown rice. Finally, each brown rice sample was milled to 90.5 ± 0.2% of milling degree. Milled rice AC reference values (AC_{ref}), transmittance NIR spectra, and physicochemical properties were combined to develop the dual-step calibration model. The raw NIR transmittance spectra was preprocessed by applying a 2nd order Savitzky-Golay derivative with a 2nd polynomial order. Later, AC_{ref} values, transformed NIR spectra, and physicochemical properties were analyzed by partial least squares regression (PLS) and multiple linear regression (MLR) to develop an accurate dual-step calibration model. Our dual-step calibration model described low and ordinary amylose varieties models, which were developed individually. Both the low and ordinary amylose varieties models were calibrated using 2008-2017 production year samples (n = 903) and validated by distinct 2018 production year samples (n = 33), which were collected at a rice grain elevator. Next, the dual-step calibration model was created by merging the validation results of the low and ordinary amylose varieties models. Results indicated that AC_{ref} values were determined with high accuracy based on the low average standard error of the laboratory method (SEL) = 0.17% among varieties and production years. Also, the regression coefficients of each wavelength related to AC_{ref} for the optimal PLS factor indicated that the wavelength at 916 nm reported the highest spectral variation and thus correlated the most to AC. Moreover, validation statistics such as standard error of prediction (SEP) = 0.33% and ratio of performance deviation (RPD) = 5.09 indicated the high robustness and accuracy of the dual-step model, enabling more precise, accurate, and efficient rice quality screening at Japanese grain elevators.

Keywords: *Oryza sativa* L., Amylose content, Near-infrared spectroscopy, Chemometric analyses, Quality, Practical application

ACKNOWLEDGEMENTS

This research was supported by a grant from the project of the National Agriculture and Food Research Organization (NARO) in Japan, Bio-oriented Technology Research Advancement Institution (BRAIN) titled the special scheme project on vitalizing the management entities of agriculture, forestry, and fisheries.

Oral Session | Postharvest/Food Technology and Process Engineering
[6-1015-C] Postharvest/Food Technology and Process Engineering (6)
Fri. Sep 6, 2019 10:15 AM - 11:30 AM Room C (3rd room)

[6-1015-C-05] Cow Milk Progesterone Concentration Determination during Milking Using Near-infrared Spectroscopy

*Patricia Nneka Iweka[1], Shuso Kawamura[1], Tomohiro Mitani[2], Takashi Kawaguchi[3], Shigenobu Koseki[1] (1. Hokkaido Univ.(Japan), 2. Field Sc. Center(Japan), 3. Orion Mach.(Japan))

Keywords: Bovine milk, Progesterone, Estrus status, Pregnancy diagnosis, Trend monitoring, Near-infrared spectroscopy, Automatic milking system

In the current dairy industry, an intensive demand for estrus detection and early diagnosis of pregnancy has been increasing. Progesterone is a steroid hormone that is secreted from corpus luteum into bovine blood and milk, and has a role of maintenance of estrus cycle and pregnancy. Therefore, progesterone concentration in cow milk is used as an important indicator of estrus detection and early diagnosis of pregnancy. Current method for milk progesterone determination requires a hormone extraction procedure that is time consuming, various types of instruments, reagents management, and various assay methods that are destructive in nature. In contrast, near-infrared spectroscopy (NIRS) is a time saving and non-destructive analytical method that can be used for online real-time determination of milk constituents content such as milk fat, protein, lactose, milk urea nitrogen and somatic cell count. However, there has been limited study on using NIRS for online real-time determination of progesterone concentration in milk during milking. Thus, the objective of this study was to develop an online real-time NIR spectroscopic sensing system for milk progesterone determination during milking by using a specific enzyme immunosorbent assay as a reference (chemical) method. Milk spectra with a wavelength range of 700 to 1050 nm and milk samples were collected every 20 s during milking from four lactating Holstein cows for 28 days using the NIR spectroscopic sensing system. Calibration models were developed using partial least squares analytical method and the precision and accuracy of the models was validated. Milk progesterone concentration for each milking was calculated by taking the progesterone concentration of the milk predicted values and milk yield obtained every 20 s, and was compared with the milk progesterone concentration chemical analysis value for one milking (bucket milk). The results obtained show that the measurement accuracy for one milking of milk progesterone concentrations was reasonably good. By installing the NIR spectroscopic sensing system developed in this study into an automatic milking system, it could predict milk progesterone concentration for one milking with almost the same accuracy as chemical analysis. Therefore, taking records of predicted values at every milking time and monitoring the continuous change of the milk progesterone concentrations, it would be possible to use this information for the detection of estrus status and diagnosis of pregnancy of each cow.

Cow Milk Progesterone Concentration Determination during Milking Using Near-infrared Spectroscopy

Patricia Iweka[1], Shuso Kawamura[*1], Tomohiro Mitani[2], Takashi Kawaguchi[3], Shigenobu Koseki[1]

[1]Laboratory of Agricultural and Food Process Engineering,
Graduate School of Agricultural Science, Hokkaido University, Japan
[2]Field Science Center for Northern Biosphere, Hokkaido University, Japan
[3]ORION Machinery CO., LTD., Japan

* Corresponding author. Email: shuso@bpe.agr.hokudai.ac.jp

ABSTRACT

In the current dairy industry, an intensive demand for estrus detection and early diagnosis of pregnancy has been increasing. Progesterone is a steroid hormone that is secreted from corpus luteum into bovine blood and milk, and has a role of maintenance of estrus cycle and pregnancy. Therefore, progesterone concentration in cow milk is used as an important indicator of estrus detection and early diagnosis of pregnancy. Current method for milk progesterone determination requires a hormone extraction procedure that is time consuming, various types of instruments, reagents management, and various assay methods that are destructive in nature. In contrast, near-infrared spectroscopy (NIRS) is a time saving and non-destructive analytical method that can be used for online real-time determination of milk constituents content such as milk fat, protein, lactose, milk urea nitrogen and somatic cell count. However, there has been limited study on using NIRS for online real-time determination of progesterone concentration in milk during milking. Thus, the objective of this study was to develop an online real-time NIR spectroscopic sensing system for milk progesterone determination during milking by using a specific enzyme immunosorbent assay as a reference (chemical) method. Milk spectra with a wavelength range of 700 to 1050 nm and milk samples were collected every 20 s during milking from four lactating Holstein cows for 28 days using the NIR spectroscopic sensing system. Calibration models were developed using partial least squares analytical method and the precision and accuracy of the models was validated. Milk progesterone concentration for each milking was calculated by taking the progesterone concentration of the milk predicted values and milk yield obtained every 20 s, and was compared with the milk progesterone concentration chemical analysis value for one milking (bucket milk). The results obtained show that the measurement accuracy for one milking of milk progesterone concentrations was reasonably good. By installing the NIR spectroscopic sensing system developed in this study into an automatic milking system, it could predict milk progesterone concentration for one milking with almost the same accuracy as chemical analysis. Therefore, taking records of predicted values at every milking time and monitoring the continuous change of the milk progesterone concentrations, it would be possible to use this information for the detection of estrus status and diagnosis of pregnancy of each cow.

Keywords: Bovine milk, Progesterone, Estrus status, Pregnancy diagnosis, Trend monitoring, Near-infrared spectroscopy, Automatic milking system

Acknowledgements: This research was supported by a grant from the project of the National Agriculture and Food Research Organization (NARO) in Japan titled On-farm Demonstration Trials of Smart Agriculture.

Oral Session | Others (including the category of JSAM and SASJ)

[6-1015-D] Other Categories (3)

Chair:Takahiro Orikasa(Iwate University, Japan)

Fri. Sep 6, 2019 10:15 AM - 11:30 AM Room D (4th room)

[6-1015-D-01] Field Representation and Path Planning for Robot Tractors

*Hao Wang[1], Noboru Noguchi[1] （1. Hokkaido University(Japan)）

10:15 AM - 10:30 AM

[6-1015-D-02] Driving Force Control for Suppression of Tractor’ s Dynamic Pitching Angle

*Yuya Aoyagi[1], Masami Matsui[2] （1. Tokyo University of Agriculture and Technology (Japan), 2. Utsunomiya University(Japan)）

10:30 AM - 10:45 AM

[6-1015-D-03] Development of a Smart Spraying System For Weeds On Rice Fields

*Thanh Tinh Nguyen[1], Ricardo Ospina[2], Noboru Noguchi[2] （1. Hokkaido University, Graduate School of Agriculture(Japan), 2. Hokkaido University, Research Faculty of Agriculture(Japan)）

10:45 AM - 11:00 AM

[6-1015-D-04] Deep Learning and Multiple Sensors Data Acquisition System for Real-time Decision Analysis in Agriculture Using Unmanned Aerial Vehicle

*Yunyan Xie[1], Ryozo Noguchi[2], Tofael Ahamed[2] （1. Graduate School of Life and Environmental Sciences, University of Tsukuba(Japan), 2. Faculty of Life and Environmental Sciences, University of Tsukuba(Japan)）

11:00 AM - 11:15 AM

[6-1015-D-05] Autonomous Navigation and Obstacle Avoidance for a Robotic Mower using Machine Vision

*Kosuke Inoue[1] （1. The University of Tokyo(Japan)）

11:15 AM - 11:30 AM

10:15 AM - 10:30 AM (Fri. Sep 6, 2019 10:15 AM - 11:30 AM Room D)

[6-1015-D-01] Field Representation and Path Planning for Robot Tractors

*Hao Wang[1], Noboru Noguchi[1] (1. Hokkaido University(Japan))

Keywords: Smart agriculture, Agricultural robots, Path planning, Headland turning, Minimum bounding box

An optimal coverage path planning method is presented to improve field efficiency; and in particular, to fully utilize the advantages provided by automatically guided farming equipment. In addition, several transfer paths are created to optimize the non-working distance and time consumption. To use the merit of agricultural robots, the backward movement along the navigation path is proposed in this research. Refiling or emptying the machine is not considered in this autonomous path planning. When a non-convex field is divided into several convex sub-fields, each sub-area has to be visited once without discard. The algorithm calculates an optimal working direction and order of sub-field to decrease the non-working area. In addition, the navigation path in this study consists of two parts; one is navigation points, which distribute in the area of the farm as an array. The other part is the code indicating the settings of the tractor and the operations at that position. The coding mechanism is informative enough for complex scenarios.

Oral Session | Others (including the category of JSAM and SASJ)
[6-1015-D] Other Categories (3)
Fri. Sep 6, 2019 10:15 AM - 11:30 AM Room D (4th room)

[6-1015-D-02] Driving Force Control for Suppression of Tractor's Dynamic Pitching Angle

*Yuya Aoyagi[1], Masami Matsui[2] (1. Tokyo University of Agriculture and Technology (Japan), 2. Utsunomiya University(Japan))

Keywords: Tractor, Traveling simulation, Torque control, Prevent accident, Suppression for attitude angle

In recent years, Japan's agricultural industry has had the highest mortality rate among all other industries. The agricultural industry has also become one of the most dangerous in other countries, and this is becoming a serious problem worldwide. In Japan, the highest number of fatalities (approximately 100 fatalities per annum) result from accidents involving tractors, with the most common being rollovers. Overturning accidents can occur either when a tractor is traveling along sloped, rough terrain because the uneven road surface increases the dynamic pitch angle beyond the overturning limit, or when the operator loses control as a result of the front wheels bouncing. To prevent these accidents, it is important to control the pitch angle when traveling along such terrain. In a previous study on the attitude stabilization of vehicles while they are being driven, attitude control technology using driving torque was developed. This technology improves riding comfort in automobiles traveling along paved roads. By applying such control to a tractor, it is expected that pitching overturn accidents can be prevented. In this scenario, it is important to confirm the dynamic effect on the pitching suppression by driving torque control. Overall, in this study, a three degrees-of-freedom, vertical, pitching, and forward/backward movement behavior model of a tractor that considers the influence of the driving force on the pitch angle was developed. The reaction force that each wheel received from the road surface was calculated, and numerical calculations were performed for the acceleration along each degree of freedom. The feedback control system had a static pitch angle on the input terrain as the target value, which was applied to the model. In the control system, using PID control, the driving force was calculated from each term (proportional, integrated, and derivative) of deviations, which consist of the difference between the target value and the dynamic pitch angle. The coefficients of the PID system were determined to become effective for this condition. The limits of the driving force were set according to the specification value of the tractor engine power and the power required for slope climbing. Driving simulation using the topographic information on a site of an actual tractor overturn accident was performed with both the driving-force control model and the constant-speed traveling model. The suppression of the pitch angle by controlling the driving force was examined through a comparative analysis of the results. The pitch angle of the driving-force control model was smaller than that of the constant-speed traveling model, enabling travel along the terrain. Thus, dynamic pitch angle control was implemented and validated. The maximum pitch angle of the driving-force control model was approximately 10% smaller than that of the constant-speed traveling model. In addition, a driving force corresponding to the attitude was generated within the usable driving-force range. Pitch angle suppression was confirmed by controlling the driving force. In our study, driving simulation using topographical information on the actual accident site was conducted to examine the suppression of the dynamic pitch angle by driving-force control. Consequently, the pitch angle of the driving-force control model enabled travel along the terrain. The maximum pitch angle of the control model was approximately 10% smaller than that of the constant-speed traveling model. The results suggest that the attitude angle can be suppressed by driving-force control to prevent tractor rollover accidents.

Driving Force Control for the Suppression of the Dynamic Pitching Angle of Tractors

Yuya AOYAGI[1], Masami MATSUI[2*]

[1] Faculty of Agriculture, Tokyo University of Agriculture and Technology (Utsunomiya University), 350, Mine, Utsunomiya city, Tochigi pref. 321-8505, Japan
[2] Faculty of Agriculture, Utsunomiya University, 350, Mine, Utsunomiya city, Tochigi pref. 321-8505, Japan

*Corresponding author: m-matsui@cc.utsunomiya-u.ac.jp

ABSTRACT

In recent years, Japan's agricultural industry has had the highest mortality rate among all other industries. Further, the agricultural industry has become one of the most dangerous in other countries; this is becoming a serious problem worldwide. In Japan, the highest number of fatalities (approximately 100 fatalities per annum) are due to accidents involving tractors, with the most common being rollovers. Overturning accidents can occur either when tractors are traveling along a sloped, rough terrain because uneven road surfaces increase the dynamic pitch angle beyond the overturning limit, or when the operator loses control owing to the bouncing of the front wheels. To prevent these accidents, the pitch angle should be controlled when traveling along such terrains. By applying attitude control using driving torque to a tractor, pitching overturn accidents could be prevented. In such scenarios, the dynamic effect on the pitching suppression by driving torque control should be verified. Overall, in this study, a three degrees-of-freedom, vertical, pitching, and forward/backward movement behavior model of a tractor that considers the influence of the driving force on the pitch angle was developed. The feedback control system had a static pitch angle on the input terrain as the target value, which was applied to the model. In the control system, using Proportional-Integral-Differential (PID) control, the driving force was calculated from each term (proportional, integrated, and derivative) of deviations, which comprises the difference between the target value and the dynamic pitch angle. The coefficients of the PID system were effective under this study's condition (mechanical specifications and topographical information, etc.). The limits of the driving force were set according to the specification value of the tractor engine power and power required for slope climbing. A driving simulation using the topographic information on a site of an actual tractor overturn accident was conducted with both the driving-force control and constant-speed traveling models. The suppression of the pitch angle by controlling the driving force was examined through a comparative analysis of the results. The pitch angle of the driving-force control model was smaller than that of the constant-speed traveling model, enabling travel along the terrain. Thus, dynamic pitch angle control was implemented and validated. The maximum pitch angle of the driving-force control model was approximately 10% smaller than that of the constant-speed traveling model. In addition, a driving force corresponding to the attitude was generated within the usable driving-force range. Pitch angle suppression was confirmed by controlling the driving force. In our study, a driving simulation using topographical information on the actual accident site was conducted to examine the suppression of the dynamic pitch angle by driving-force control. Consequently, the pitch angle of the driving-force control model enabled travel along the terrain. The maximum pitch angle of the control model was approximately 10% smaller than that of the constant-speed traveling model. The results suggest that the attitude angle can be suppressed by controlling the driving force to prevent tractor rollover accidents.

Keywords: Tractor, Traveling simulation, Torque control, Prevent accident, Suppression for attitude angle

1. INTRODUCTION

In recent years, with the development of agricultural machinery, working efficiency has considerably improved and labor burden significantly reduced. However, there are approximately 350 annual cases of fatal farm accidents in Japan, indicating a high accident rate (JMAFF, 2019). In addition, the fatal

injury rate per 100,000 farmers is as high as 24.0 people in the US (USDL, 2017), 16.1 people in Japan (JMAFF, 2015), and 9.2 people in the UK (HSE, 2019). Thus, in advanced countries with mechanized agriculture, agricultural injury rates are at a high level compared with other industries. This indicates that there may be more lives being lost in areas even beyond the scope of the surveys. The agricultural industry is becoming the most dangerous industry among all industries, increasingly becoming a serious problem worldwide. Therefore, taking adequate measures to reduce the fatalities is not only an important issue but also an urgent issue.

In Japan, the highest number of fatalities (approximately 100 fatalities per annum) is due to tractor accidents and the most common cause is overturning of tractors. Because of the terrain, most tractors in Japan have to travel on rough and steep slopes. This can increase the dynamic pitching angle with the risk of exceeding the overturn angle or steering control loss. To prevent such fall accidents of tractors, it is important to control the pitching angle when traveling on rough and steep terrains. This is achieved by applying the attitude control technology that inputs the driving torque to the tractor. However, it is important to verify theoretically the pitching suppression effect.

Previous studies on tractor behavior have analyzed the simulation of tractor stability on a rigid slope (Li et al., 2016) and impact dynamics model for nonlinear bouncing of tractors (Watanabe et al., 2017). Further, an analysis of tractor pitching based on an actual accident site (Matsui et al., 2016) has also been conducted. In addition, for vehicles traveling on paved roads, research on how to vary the drive torque and stabilize the vehicle attitude to improve driving comfort has been conducted (Takahashi et al., 2016, Sugai, 2016, Sawada et al., 2005). However, although there are studies on behavior stability analysis of tractors and posture stabilization in vehicles traveling on pavements, there are a few studies on posture stabilization in agricultural machines traveling on agricultural roads (rough and steep slopes). Therefore, in this study, a dynamic simulator of a tractor with three degrees of freedom (vertical, pitching, and horizontal) was developed, considering the influence of driving force on pitching. The feedback control system was applied to the model (dynamic simulator) and static pitching angle on the input terrain was set on the target value for the system. The driving force control and constant speed models were run using topographical information of the actual accident site, the results were compared, and the pitching angle suppression effect by the driving force control was examined.

2. MATERIALS AND METHODS

Dynamic equations with three degrees of freedom (vertical, pitching, and horizontal) for the tractor were formulated considering the influence of the driving force on the pitching. The behavior model of the tractor is shown in Fig. 1.

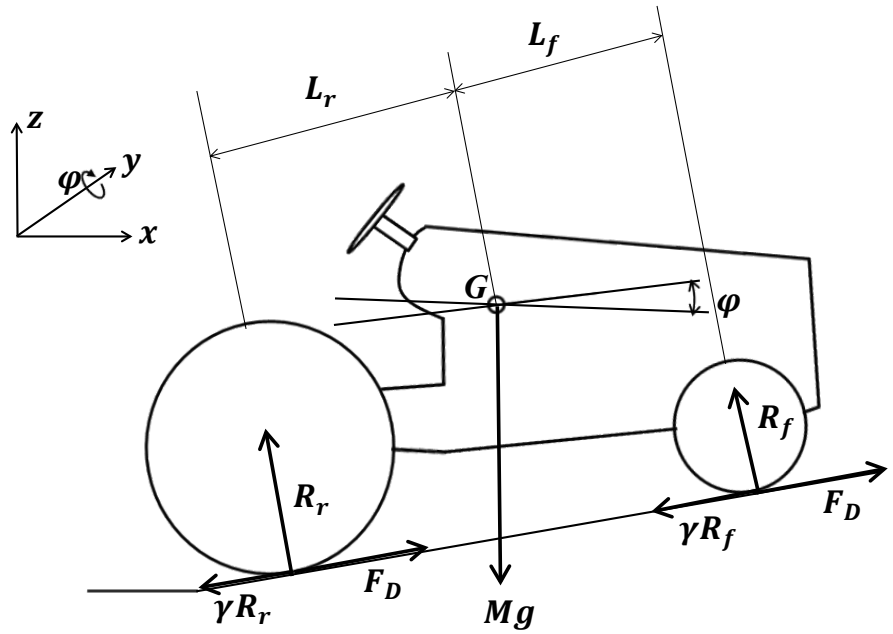

Figure 1. Behavior model of the tractor

Equations (1) to (3) provide the dynamic equations for the three degrees of freedom for the tractor. Equations (4) and (5) provide the wheel reaction and driving forces, respectively.

$$M\ddot{z} = Mg - \left(R_{fr} + R_{fl} + R_{rr} + R_{rl}\right)\cos\varphi + \gamma\left(R_{fr} + R_{fl} + R_{rr} + R_{rl}\right)\sin\varphi - F_D \sin\varphi \quad (1)$$

$$I_y\ddot{\varphi} = \left(R_{fr} + R_{fl}\right)L_f - \left(R_{rr} + R_{rl}\right)L_r - \gamma\left(R_{fr} + R_{fl} + R_{rr} + R_{rl}\right)L_g + F_D L_g \quad (2)$$

$$M\ddot{x} = F_D \cos\varphi - \gamma\left(R_{fr} + R_{fl} + R_{rr} + R_{rl}\right)\cos\varphi - \left(R_{fr} + R_{fl} + R_{rr} + R_{rl}\right)\sin\varphi \quad (3)$$

$$R_{ij} = (z + L_i\varphi)\, k_i + (\dot{z} + L_i\dot{\varphi})\, c_i \quad (4)$$

$$F_D(t) = K_p e(t) + K_i \int e(t)dt + K_d \frac{de(t)}{dt} \quad (5)$$

where,
$M =$ Mass of body [kg], $F_D =$ Driving force [N], $R =$ Reaction force of wheel [N],
$I_y =$ Inertia moment of pitching [kg・m^2], $k =$ Spring coefficient [N/m],
$c =$ Damping coefficient [N・s/m], $g =$ Gravity acceleration [m/s^2], $z =$ Vertical displacement [m],
$\varphi =$ Pitching angle [rad], $x =$ Horizontal displacement [m],
$L_f =$ Length of mass center to front axle [m], $L_r =$ Length of mass center to rear axle [m],
$L_g =$ Length of mass center to ground [m], $e(t) =$ Deviation of control system

Based on these dynamic equations, an original simulator using Matlab/Simulink was developed. In the simulator, the reaction force that each wheel receives from the road surface was calculated, and the acceleration for each degree of freedom was numerically calculated using the fourth-order Runge–Kutta method. The tractor specifications and model parameters are summarized in Table 1.

Table 1. Tractor specifications and model parameters

Item	Value
Body mass [kg]	1050
Full length [m]	2.98
Full width [m]	1.32
Total height [m]	1.93
Wheel base [m]	1.5
Distance of mass center and ground [m]	0.91
Distance of mass center and rear axle [m]	0.65
Kp [-]	100
Ki [-]	280
Kd [-]	20
Inertia moment of pitching [kg・m^2]	600
Front wheel spring coefficient [N/m]	60000
Front wheel damping coefficient [N・s/m]	200
Rear wheel spring coefficient [N/m]	160000
Rear wheel damping coefficient [N・s/m]	4400

The specifications used catalog values of a 30-horsepower tractor; further, the spring coefficient, damping coefficient, and moment of inertia used the values measured experimentally (Aoyagi et al., 2016).
A control system diagram is shown in Fig. 2. In the control system, using PID control, the driving force was calculated from each term (proportional, integrated, and derivative) of deviations, which comprises the difference between the target value and the dynamic pitch angle. As for control parameters, Kp, Ki, and Kd were searched in the range 1–500, respectively, and the most effective parameters of suppressing the maximum pitching angle were determined for the conditions assumed in this study. The limits of the driving force were set according to the specification value of the tractor engine power and power required for slope climbing.

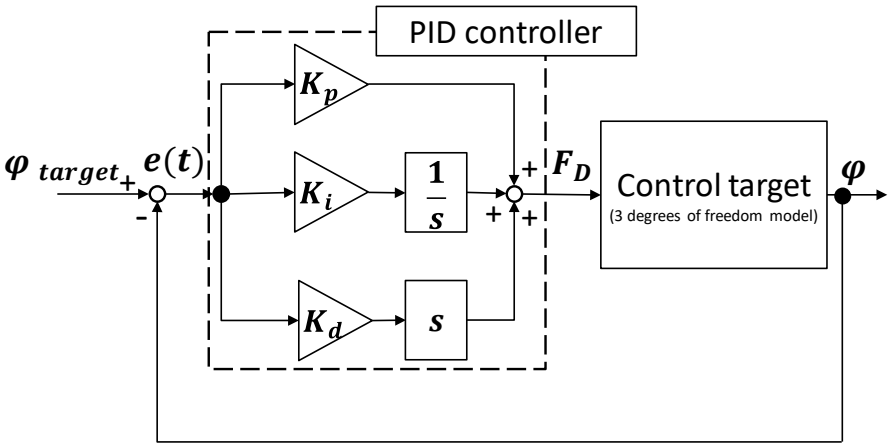

Figure 2. Control system diagram

For a simulation using the topographical information of actual accident site, we conducted a survey and hearing considering a tractor fall accident site that occurred in Niigata Prefecture in 2013 (Fig. 3).

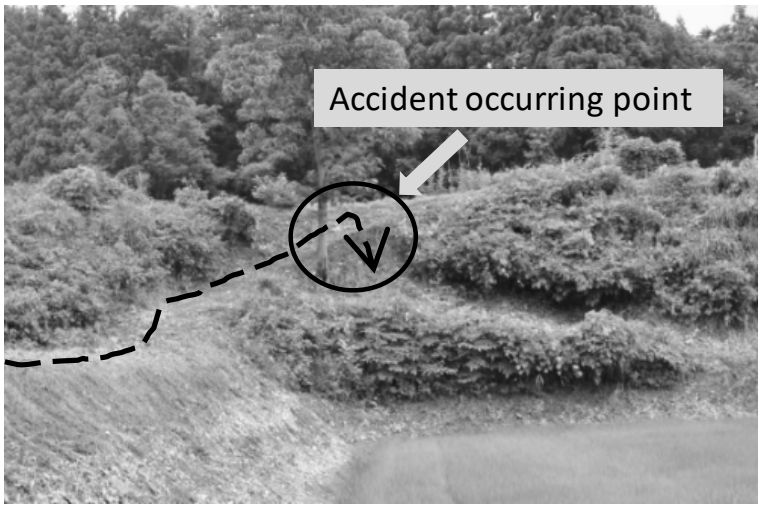

Figure 3. Accident site of the tractor

As for how the actual accident occurred, when the tractor climbed up on a farm road with a slope of about 20° at a traveling speed of about 1.0 m/s, the front wheel of the tractor bounced up and fell to the right near the middle of the slope. The input topography was reproduced by adding measured surface roughness to spline interpolation of the topography data obtained by surveying (Fig. 4).

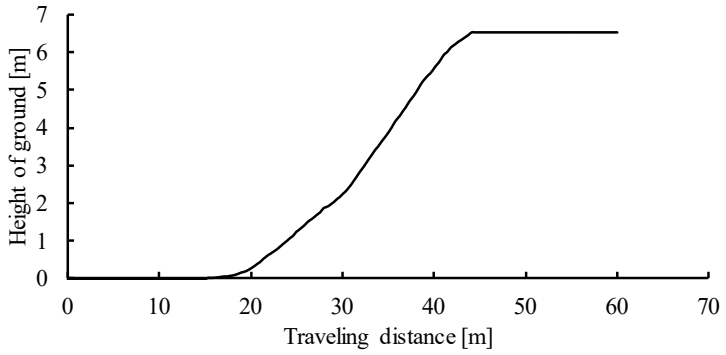

Figure 4. Input terrain

The driving simulation was conducted with the driving force control model and constant speed model, the results were compared, and the pitching angle suppression effect by the driving force control was examined.

3. RESULTS AND DISCUSSION

Fig. 5 shows the pitching displacement of the pitching angle control and constant speed models (1.0 m/s). The control effect (suppressed pitch angle) can be confirmed by observing that compared with the constant speed model, the pitching angle is suppressed for the control model. In particular, the control effect is remarkable in the traveling distance between 30 m and 40 m. The maximum pitching angle is 18.4° for the control model and 21.0° for the constant speed model around the traveling distance of 40 m. The maximum pitching angle of the control model is approximately 88% of the maximum pitching angle of the constant speed model.

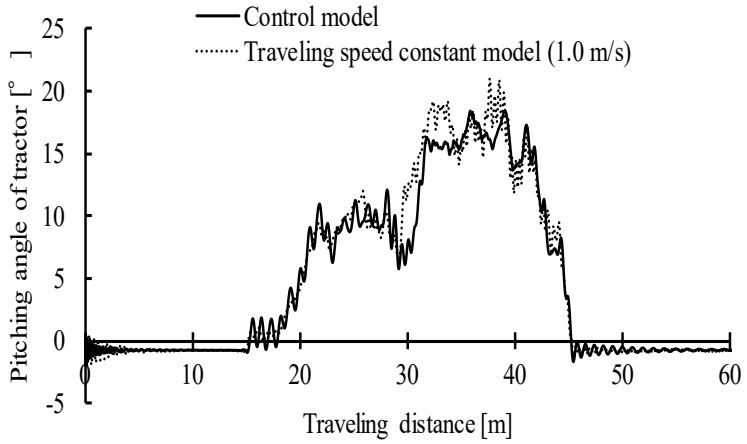

Figure 5. Pitching displacements of the control and constant speed models

Fig. 6 shows the increasing and decreasing of the pitching angle (the difference between the dynamic attitude angle and the static attitude angle) compared with the static pitching angle. Fig. 6 shows that the pitching angle is increased to a maximum of 3.7° in the control model and the pitching angle is increased at a maximum of 7.7° in the constant speed model. Moreover, the RMS value of each pitching angle increase/decrease in the travel distance between 15 m and 45 m (climbing section) is 1.9° in the control model and 2.6° in the constant speed traveling model; further, it travels more parallelly to the topography in the control model (showing a pitching angle close to the static attitude angle).

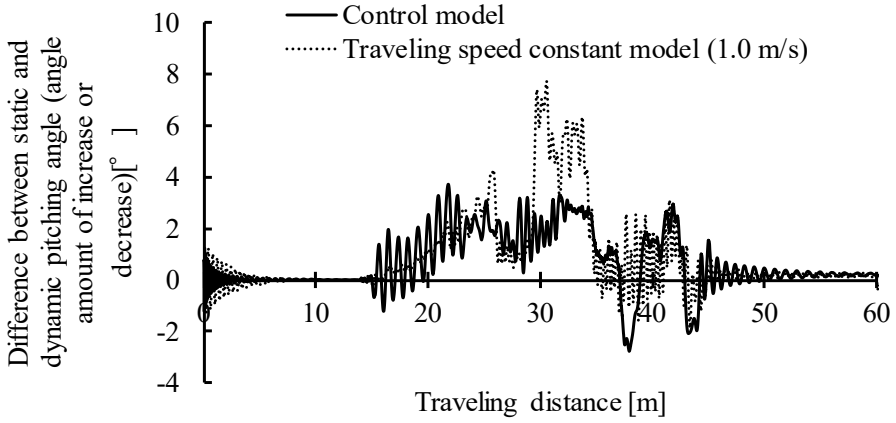

Figure 6. Fluctuations of pitching angle in comparison to static angle

Fig. 7 shows the driving force displacement of the pitching angle control model. The figure also shows that the driving force in the control model corresponds to the posture. This indicates the possibility of effectively controlling attitude by controlling the driving force according to the attitude angle.

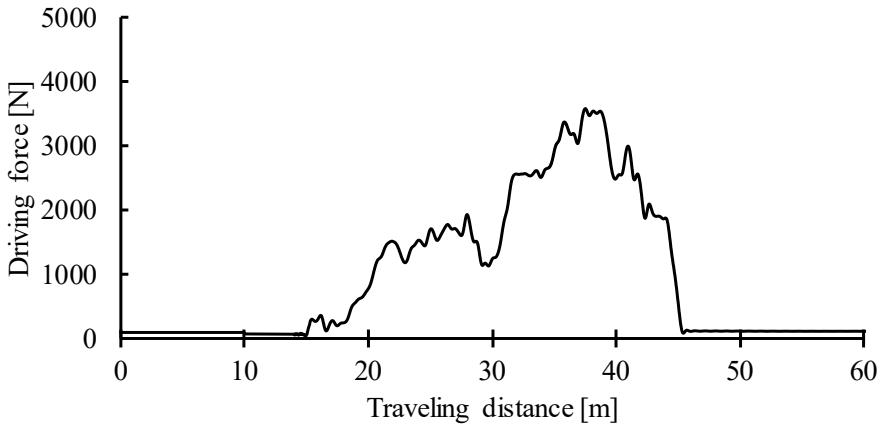

Figure 7. Driving force displacement of the control

From the above research, the suppression effect of the dynamic pitching angle by the driving force control is examined by the driving simulation based on topographical information of the actual accident site. The pitching angle suppression effect is obtained by controlling the driving force, and it was possible to travel along the terrain compared with the constant speed model. In addition, it was shown that the maximum pitching angle of the control model was approximately 10% lower than the maximum pitching angle of the constant speed model under the conditions of this study. From this, the possibility of attitude angle suppression by driving force control for fall accident prevention was shown.

4. CONCLUSION

Farm work accidents are a global issue. In Japan, the most common agricultural accident is the overturning of tractors, which require the most urgent mitigating measures. The stabilization of the posture of the tractor by drive torque control is expected to prevent pitching overturn, and it is important to theoretically verify the pitching suppression effect. In this study, a dynamic simulator with three degrees of freedom (vertical, pitching, and horizontal) of a tractor was developed considering the influence of the driving force on the pitching. The feedback control system was applied to the model (dynamic simulator) and static pitching angle on the input terrain was set on the target value for the system. The driving force control and constant speed models were run using the topographical information of the actual accident site; the results were compared, and the pitching angle suppression effect by the driving force control was examined.

As a result of this simulation, the pitching angle of the control model could be suppressed (traveling along the terrain) compared with that of the constant speed model, and the control effect can be confirmed. Furthermore, the maximum pitching angle is 18.4° for the control model and 21.0° for the constant speed model; the maximum pitching angle of the control model is about 10% lower than the constant speed model. In addition, the pitching angle of the control model rises 3.7° with respect to the static attitude and pitching angles of the constant-speed travel model rises at 7.7°, and the driving force according to the attitude is generated in the control model.

From the above research, the suppression effect of the dynamic pitching angle by the driving force control was examined by the driving simulation based on the topographical information of the actual accident site. The pitching angle suppression effect was obtained by controlling the driving force, and it was possible to travel along the terrain compared with the constant speed model. In addition, it was shown that the maximum pitching angle of the control model was about 10% lower than the maximum pitching angle of the constant speed model under the conditions of this study. From this, the possibility of attitude angle suppressing by driving force control for fall accident prevention was demonstrated.

ACKNOWLEDGMENT

This work was supported by Grant-in-Aid for JSPS Fellows JP18J13679.

REFERENCES

Aoyagi, Y., Matsui, M., Morio, D., Tamura, T., Uchikawa, Y., Kimura, T. 2016. Study on tractor behavior based on accident topography. *Journal of the Japanese Society of Agricultural Machinery and Food Engineers* 78(6):529-535.

Health and Safety Executive, 2019. Fatal injuries in agriculture, forestry and fishing in Great Britain 2018/19. http://www.hse.gov.uk/agriculture/pdf/agriculture-fatal-injuries-1819.pdf. Accessed Jul. 16, 2019.

Japan Ministry of Agriculture, Forestry and Fisheries, 2019. The aggregate results of the agricultural work fatal accident information received from the State in 2017. http://www.maff.go.jp/j/press/seisan/sizai/attach/pdf/190128-1.pdf. Accessed Jul. 16, 2019.

Japan Ministry of Agriculture, Forestry and Fisheries, 2017. Presentation about farm work safety measures in Feb. 6, 2017. http://www.maff.go.jp/j/seisan/sien/sizai/s_kikaika/anzen/attach/pdf/2017_spring_suisin-5.pdf. Accessed Jul. 16, 2019.

Matsui, M., Aoyagi, Y., M., Morio, D., Tamura, T., Uchikawa, Y., Kimura, T. 2017. Study on tractor behavior based on accident topography: swing mechanism modeling of front axle and influence of mass center position on anteroposterior fall. *Journal of the Japanese Society of Agricultural Machinery and Food Engineers* 79(1):59-65.

Sawada, M., Matsumoto, H. (DENSO Co.) 2005. Vehicle stabilization control system. Japanese Patent No. 2005-256636 (In Japanese).

Sugai, T. (NTN Co.) 2016. Vehicle attitude control device. Japanese Patent No. 2016-199195 (In Japanese).

Takahashi, S., Katsuyama, E. (TOYOTA Co.) 2016. Vehicle control device. Japanese Patent No. 2016-25783 (In Japanese).

U.S. Department of Labor, 2017. National census of fatal occupational injuries in 2017. https://www.bls.gov/news.release/pdf/cfoi.pdf. Accessed Jul. 16, 2019.

Watanabe, M., Sakai, K. 2017. Impact dynamics model for a nonlinear bouncing tractor during inclined passage. *Journal of Biosystems Engineering* 79(2):149-157.

Zhen, L., Mitsuoka, M., Inoue, E., Okayasu, T., Hirai, Y. 2015. Development of stability indicators for dynamic Phase I overturn of conventional farm tractors with front axle pivot. *Biosystems Engineering* 34(1):55-67.

Oral Session | Others (including the category of JSAM and SASJ)
[6-1015-D] Other Categories (3)
Fri. Sep 6, 2019 10:15 AM - 11:30 AM Room D (4th room)

[6-1015-D-03] Development of a Smart Spraying System For Weeds On Rice Fields

*Thanh Tinh Nguyen[1], Ricardo Ospina[2], Noboru Noguchi[2] (1. Hokkaido University, Graduate School of Agriculture(Japan), 2. Hokkaido University, Research Faculty of Agriculture(Japan))

Keywords: Precision agriculture, Weeds, Rice field, Image processing, Real time detection

In recent years, precision agriculture has become an important aspect of sustainable agriculture and environment protection. The problem of how to reduce the amount of chemicals used on the fields while ensuring productivity has become a challenge. In this study, we developed a smart spraying system prototype which uses a machine vision system capable of performing real time detection of two kinds of weeds in the paddy fields of the Vietnamese Mekong Delta (VMD). The prototype of the smart spraying system was tested to perform real time precision spraying of herbicide on weed location. The input images were recorded by using an RGB camera. The discrimination between rice and weeds was obtained by processing the images based on well-known image segmentation methods and analysis of the bounding rectangle of blob. This method is simple but effective, allowing to detect narrow leaf weeds and broadleaf weeds on the post-emergence stage of weeds with reasonable accuracy. Accuracy of spraying was also evaluated, spray volume and rate application were adapted and tuned for real work conditions on the field. Results suggest this system is more precise and reliable in comparison to current methods used in Vietnam.

Development of a Smart Spraying System For Weeds On Rice Fields

Thanh Tinh Nguyen[1], Ricardo Ospina[2], Noboru Noguchi[*]

[1]Graduate School of Agriculture, Hokkaido University, Kita-9, Nishi-9, Kita-Ku, Sapporo, Hokkaido, 060-8589, Japan.
[2]Research Faculty of Agriculture, Hokkaido University, Kita-9, Nishi-9, Kita-Ku, Sapporo, Hokkaido, 060-8589, Japan.
[*]Corresponding author, Research Faculty of Agriculture, Hokkaido University, Kita-9, Nishi-9, Kita-Ku, Sapporo, Hokkaido, 060-8589, Japan. E-mail address: noguchi@bpe.agr.hokudai.ac.jp.

ABSTRACT

In recent years, precision agriculture has become an important aspect of sustainable agriculture and environment protection. The problem of how to reduce the amount of chemicals used on the fields while ensuring productivity has become a challenge. In this study, we developed a smart spraying system prototype which uses a machine vision system capable of performing real time detection of two kinds of weeds in the paddy fields of the Vietnamese Mekong Delta (VMD). The prototype of the smart spraying system was tested to perform real time precision spraying of herbicide on weed location. The input images were recorded by using an RGB camera. The discrimination between rice and weeds was obtained by processing the images based on well-known image segmentation methods and analysis of the bounding rectangle of blob. This method is simple but effective, allowing to detect narrow leaf weeds and broadleaf weeds on the post-emergence stage of weeds with reasonable accuracy. Accuracy of spraying was also evaluated, spray volume and rate application were adapted and tuned for real work conditions on the field. Results suggest this system is more precise and reliable in comparison to current methods used in Vietnam.

Keywords: Precision agriculture, Weeds, Rice field, Image processing, Real time detection.

1. INTRODUCTION

Agriculture production in Vietnam is facing increasing environmental impacts due to large amounts of herbicide used in various species of crops. According to the International survey of herbicide resistant weeds (Heap, 2019), the types of herbicide and site application have been increasing year by year and continue to enlarge. This is because agriculture needs to increase productivity and quantity to cover the food demands for a population of more than 7 billion all over the world. Vietnam is an agriculture-based country and a top rice exporter in the world market. The country has 65 percent of cultivated land area ranging from the north to the south; especially in the Mekong Delta, which is the biggest cultivated region in Vietnam. The government has issued many especial policies oriented to increase rice quantity and productivity (Dung et al., 1999). However, using a large amount of pesticides causes damage to the environment, the human health and effects sustainable agriculture.

Some recent researches show hard conditions for detection of plants mixed with weeds by using deep learning CNN algorithms (Barrero et al., 2016; dos Santos Ferreira et al., 2017). However, these algorithms show low accuracy with small object detection and processing time is not good for real time applications. Thus, current research applications for crops only distinguish between weeds and crop rows. In this study, a machine vision method based on bounding blob that can classify crops and weeds is introduced. This method can detect two kinds of weeds native from the rice fields of the VMD. Besides, a real-time spraying prototype was developed for evaluation of the detection and spraying system.

2. MATERIALS AND METHODS

2.1. Image processing

The common weeds present in rice fields in Vietnam are not different from common weeds along Asia. There are several types of commercial herbicides available based on the biological characteristics of weeds. Typically, there are two main kinds of weeds present on the rice fields of the Vietnam Mekong Delta (VMD); which can be classified as broadleaf and narrow leaf (including grasses and sedges) types(Caton et al., 2010). There are three stages during the crop growth that allow application of the herbicide (IRRI, 2018). However, some stages require a high amount of herbicide; causing pollution of the environment. Sometimes weeds are mature, so it is necessary to apply a stronger type of herbicide at a higher rate. Higher concentrations of herbicide will affect and even may destroy the rice plants, particularly in the panicle initiation and flowering of rice stages. The field condition during the post-emergence stage of the crop growth is shown in Figure 1. At that time, the rice plant is in the stage of 7-10 days after sowing. Figure 1 shows not only the different colors, but also the different sizes between rice and weeds.

Figure 1. Weed post-emergence.

Figure 1 also shows how rice leaves and weed leaves do not overlap together. Therefore, for this particular research this is a good condition to apply image processing for segmentation between weed, soil and rice.

The image processing algorithm flow chart is shown on Fig. 2. OpenCV library for C++ language was used to make the program. Each step in the flow chart is explained in detail as follow.

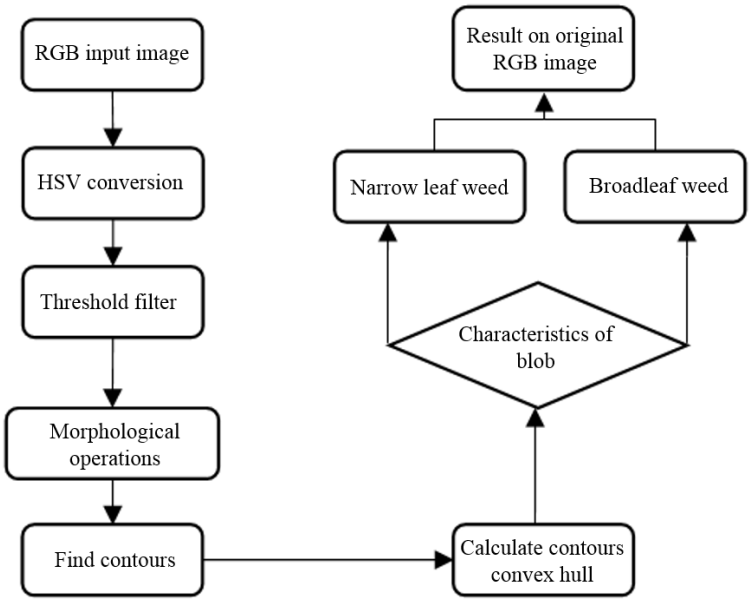

Figure 2. Algorithm of weed detection.

The input RGB image recorded by a camera is converted into the HSV color space for image segmentation. Then, a threshold filter is used to separate soil from vegetation, giving as a result a binary image. Morphological operations of dilation and erosion are applied to the binary image to smooth the noise and make the border of the plants look clear. Then, the contours of all the white regions on the image are detected. Calculation of the convex hull is performed on each detected contour in order to find the smallest convex set of points that can represent each contour on the image. Then, the bounding rectangle of each the contours is used to analyze the characteristics of each plant; as show in Figure 3. Such characteristics include the area of the bounding rectangle (S_r), the ratio between the height (h) and the width (w) of the bounding rectangle, the diagonal (d), and the ratio between the area of the contour (S_c) and its corresponding bounding rectangle. These characteristics help to remove the rice and remaining noises from the image. The setting values for detection between the narrow leaf and broadleaf weed are different. The ratio S_c/S_r is particularly helpful to distinguish the kind of weeds. Finally, the algorithm counts and labels each type of weed, with yellow for broadleaf weed and green for narrow leaf weed, as shown in Figure 4.

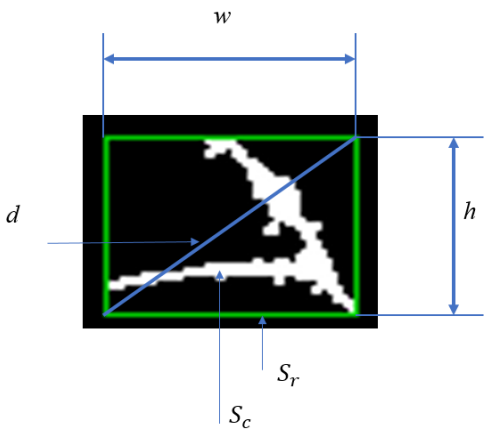

Figure 3. Bounding rectangle characteristics for blob analysis.

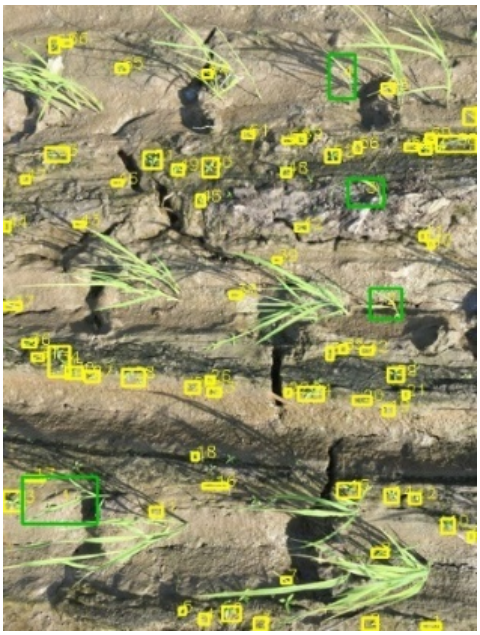

Figure 4. Result of narrow leaf and broadleaf weed detection on original image.

2.2. Prototype of sprayer

A sprayer prototype was built for this study with the purpose of testing the effectiveness of the detection algorithm and explore the possibility of implementing into real life applications. Since the algorithm can detect two different types of weeds, two different types of herbicide can be applied. Figure 5 a) shows the full design in 3D and Figure 5 b) shows the real prototype. The prototype was built up on a steel table (0.9m length, 0.7m width, 0.8m height) which can move smoothly on 4 wheels placed on its legs.

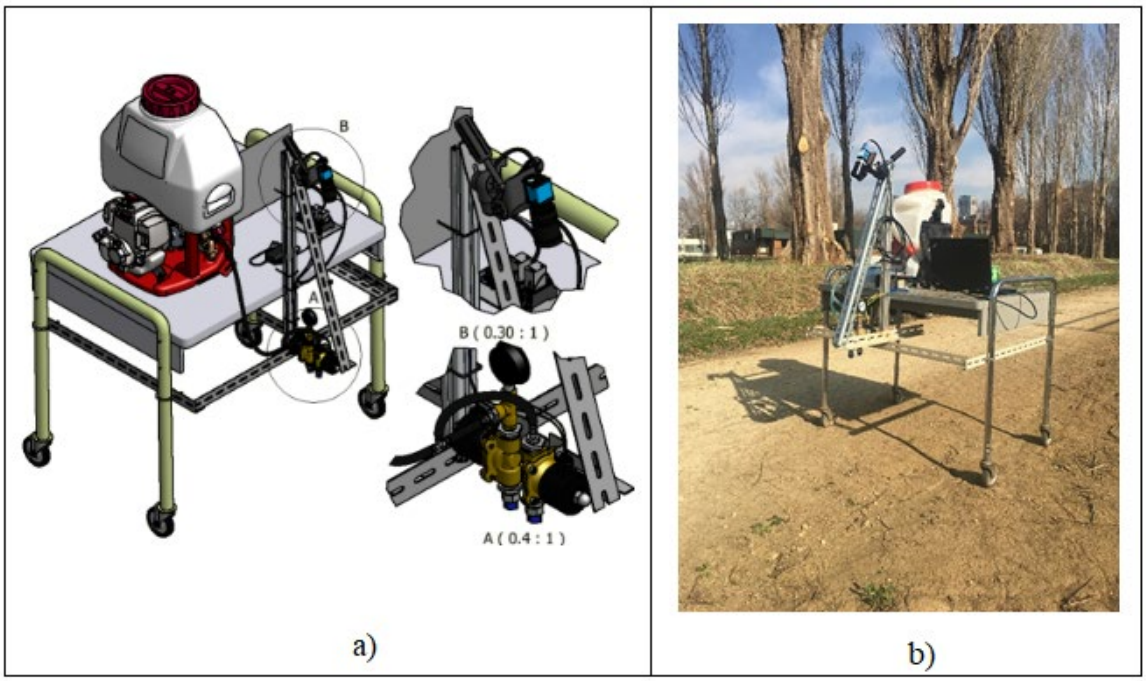

Figure 5. Sprayer prototype. a) Prototype on 3D design by Inventor software. b) Real prototype.

All the components and equipment of the prototype are shown on Figure 6; the camera is used to get image frames; an Arduino Uno is used as a controller and a backpack sprayer is used to control the spraying pressure. When the image processing algorithm detects the weed, the program will send a command to the Arduino Uno to activate the output signal to control the solenoid valve of the sprayer.

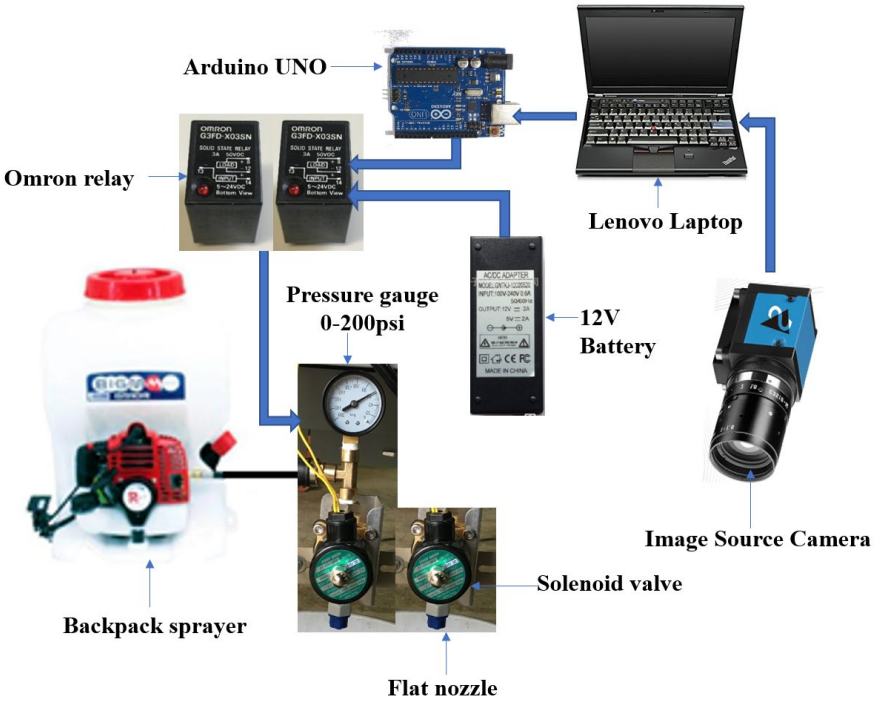

Figure 6. Accessories equipment and connection diagram of prototype.

3. RESULTS AND DISCUSSION

To evaluate the accuracy of the detection algorithm we used 112 RGB images, which were taken from real conditions on rice field in Vietnam. The real results were calculated for each sample picture based on an expert criterion, counting the weeds and rice plants. In this study, the linear regression method was used to evaluate the similarity between the detected values and the real values. Figure 8 a) shows the detection evaluation for broadleaf weed. Figure 8 b) shows the detection evaluation for narrow leaf weeds. In this experiment, it was show that the detection of broadleaf weeds has a higher accuracy than the detection of narrow leaf weed. The explanation for this result is because the broadleaf weed has a clear different size and shape compared to rice. However, the narrow leaf weed is not too much different.

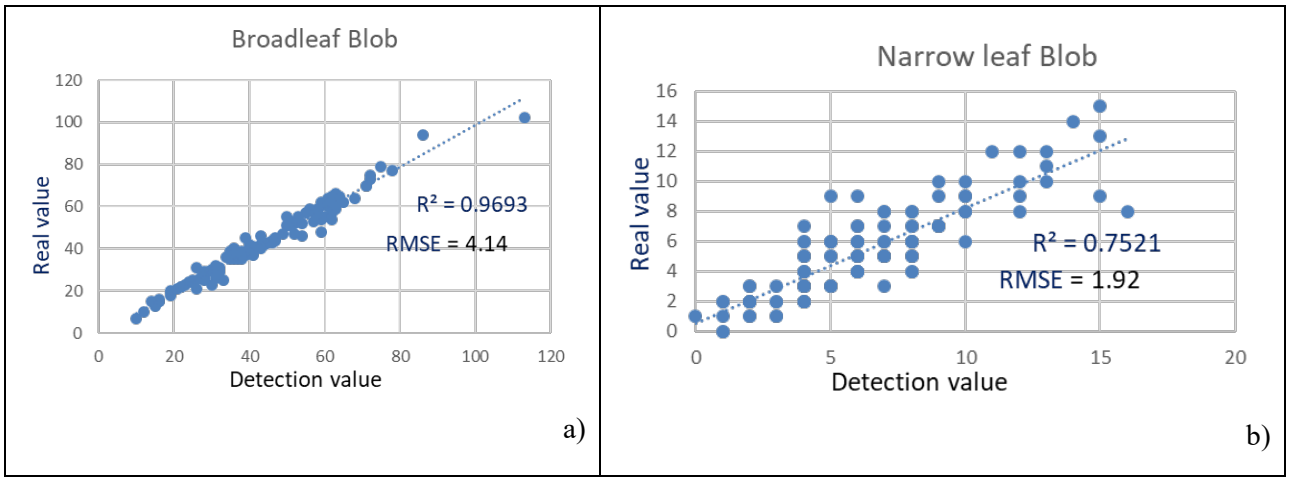

Figure 7. Weeds detection evaluation. a) Broadleaf weeds. b) Narrow leaf weeds.

For evaluation of the real time sprayer, the prototype was tested inside a laboratory because it is not suitable to use in the real rice field. The laboratory with cement floor can help to obtain a smooth movement without vibration, the indoor electric lighting system helps to balance light conditions for testing. Two types of weed samples were used. The size and shape of the samples is similar to the weeds found in Vietnam. The physical characteristics of the weed samples were carefully verified based on an expert criterion. The two kinds of the weed's samples were arranged in a random order in a straight line. Figure 9 shows the result of detection and spraying. When the prototype moves forward at 0.67 m/s, the nozzles spray at the correct position on each weed location; the water amount of each sprayer is 0.0048 liter. The resulting frame rate for the image processing algorithm is 10 FPS (Frame per second), and the delay time from the detection to nozzle sprayer activation is 0.35 seconds. Considering the traveling speed of the prototype, this method is suitable for effective spraying in real life applications. Besides, it is also consistent with the speed of rice transplanter machines traveling in paddy fields (Sato et al., 1996).

Figure 8. Experiment result of two kinds of weeds detection and spraying.

4. CONCLUSION

The proposed combined strategy works properly when the weeds are present on an early stage of growth, which coincides with the right timing for herbicide application. If the crop is further developed, the weed

will most likely present overlapping with the leaves of rice plants and the segmentation process will become difficult. Nevertheless, the proposed approach provides a useful methodology to discriminate weeds in the real paddy field situations, which display a mixture of rice, soil and weeds over many kinds of fields used in Vietnam like transplanting field, spot seeding field, and broadcasting field. Although the results can be considered satisfactory, this method might be only applied for distinguish weeds and rice on spot seeding fields and transplanting fields. In the broadcasting fields with high density of rice, the segmentation will be low, and results might not be accurate. It is also necessary to design strategies to cope with the variability of lighting conditions, and velocity and vibration of the spraying system traveling forwards. As future work, it is proposed to improve the image processing time. Also, a new mechanical design is required to improve the balance and reduce the vibration on the camera.

REFERENCES

Barrero, O., Rojas, D., Gonzalez, C., & Perdomo, S. (2016). *Weed detection in rice fields using aerial images and neural networks.* Paper presented at the Signal Processing, Images and Artificial Vision (STSIVA), 2016 XXI Symposium on.

Caton, B. P., Mortiner, M., Hill, J. E., & Johnson, D. E. (2010). *Weed of Rice in Asia*.

dos Santos Ferreira, A., Matte Freitas, D., Gonçalves da Silva, G., Pistori, H., & Theophilo Folhes, M. (2017). Weed detection in soybean crops using ConvNets. *Computers and Electronics in Agriculture, 143*, 314-324. doi: 10.1016/j.compag.2017.10.027

Dung, N. H., & Dung, T. T. T. (1999). Economic and health consequences of pesticide use in paddy production in the Mekong Delta, Vietnam. *EEPSEA research report series/IDRC. Regional Office for Southeast and East Asia, Economy and Environment Program for Southeast Asia*.

Heap, I. (2019). The international survey of herbicide resistant weeds. *Avaible at: http://www.weedscience.org/*.

IRRI. (2018). Herbicide - when to apply, from http://www.knowledgebank.irri.org/step-by-step-production/growth/weed-management/herbicides

Sato, J.-i., Shigeta, K., & Nagasaka, Y. (1996). Automatic Operation of Light Tractor with Sprayer in Paddy Fields. *JARQ, 30*, 239-244.

11:00 AM - 11:15 AM (Fri. Sep 6, 2019 10:15 AM - 11:30 AM Room D)

[6-1015-D-04] Deep Learning and Multiple Sensors Data Acquisition System for Real-time Decision Analysis in Agriculture Using Unmanned Aerial Vehicle

*Yunyan Xie[1], Ryozo Noguchi[2], Tofael Ahamed[2] （1. Graduate School of Life and Environmental Sciences, University of Tsukuba(Japan), 2. Faculty of Life and Environmental Sciences, University of Tsukuba(Japan)）

Keywords: UAV, Machine Learning, Deep Learning, Multiple Sensors

This research was conducted to develop a user-friendly application to connect multiple sensors while using UAV to collect field data. The onboard and ground sensors were connected in the same application for ease of data collection in one software application. In the onboard sensors, thermal and RGB cameras were connected and transmitted the images within 500 m – 1000 m range. The soil moisture content information, humidity information were collected. In addition, the image analysis and deep-learning algorithm was added to the classification of the objects while landing. Histogram of Oriented Gradient (HOG) and Support Vector Machine (SVM) and YOLOV3 algorithms were implemented for classification of human, vehicle and others obstacle. The Michihibiki module was also connected with IoT application to soil moisture content measurement in the larger fields. The user application is divided into three modules: Hardware Module for Sensors Networks (HMSN), Software Module for Data Acquisition (SMDA), and Deeping Learning for Decision Analysis (DLDA). This research will be extended further with real-time analysis and decision support systems for UAV-based agricultural operations and safety systems.

Oral Session | Others (including the category of JSAM and SASJ)
[6-1015-D] Other Categories (3)
Fri. Sep 6, 2019 10:15 AM - 11:30 AM Room D (4th room)

[6-1015-D-05] Autonomous Navigation and Obstacle Avoidance for a Robotic Mower using Machine Vision

*Kosuke Inoue[1] (1. The University of Tokyo(Japan))

Keywords: Autonomous Navigation, Visual SLAM, Obstacle Avoidance, Deep Learning, Object Detection, Stereo Camera

The autonomous operation of agricultural machinery using global navigation satellite system (GNSS) information has recently experienced rapid development as a labor-saving measure in agriculture. The self position is recognized with a GNNS signal, and the vehicle can travel in the area autonomously. However, if the vehicle is driven using only the GNSS signal such that the surrounding environment is not recognized, there is a risk of collision with an obstacle. Furthermore, sensors such as radars or lasers cannot distinguish between grass and obstacles and thus cannot be used to detect the likely obstacles encountered by agricultural machinery. Autonomous driving cannot be performed in environments where the satellite positioning accuracy is low, such as orchards. Herein, an autonomous driving system was developed that performs obstacle avoidance and autonomous driving without a GNSS signal by using an object detection system that is based on a stereo camera and deep learning. Stereo cameras and convolutional neural networks recognize the environment and avoid obstacles. The self position is corrected by observing a landmark in the environment. The experiment will be conducted at the Tanashi Forest of the University of Tokyo to evaluate autonomous driving by employing real-time kinematic-GNSS to measure the true values.

Autonomous navigation and obstacle avoidance for a robotic mower using machine vision

Kosuke Inoue[1*], Yutaka Kaizu[1], Sho Igarasahi[1], Kenji Imou[1]

[1]Department of Biological and Environmental Engineering, The University of Tokyo, Japan

*Corresponding author: pdzvpa990@g.ecc.u-tokyo.ac.jp

ABSTRACT

The autonomous operation of agricultural machinery using global navigation satellite system (GNSS) information has recently experienced rapid development as a labor-saving measure in agriculture. The self position is recognized with a GNNS signal, and the vehicle can travel in the area autonomously. However, if the vehicle is driven using only the GNSS signal such that the surrounding environment is not recognized, there is a risk of collision with an obstacle. Furthermore, sensors such as radars or lasers cannot distinguish between grass and obstacles and thus cannot be used to detect the likely obstacles encountered by agricultural machinery. Autonomous driving cannot be performed in environments where the satellite positioning accuracy is low, such as orchards. Herein, an autonomous driving system was developed that performs obstacle avoidance and autonomous driving without a GNSS signal by using an object detection system that is based on a stereo camera and deep learning. Stereo cameras and convolutional neural networks recognize the environment and avoid obstacles. The self position is corrected by observing a landmark in the environment. The experiment will be conducted at the Tanashi Experimental Forest of the University of Tokyo to evaluate autonomous driving by employing real-time kinematic-GNSS to measure the true values.

Keywords: Autonomous Navigation, Visual SLAM, Obstacle Avoidance, Deep Learning, Object Detection

1. INTRODUCTION

The automation of farm operations using robot technology has increased in Japan due to the decreasing number and aging of farmers. Autonomous tractors, which can automatically perform agricultural tasks using GNSS information, have been developed. We are currently developing a robot mower that uses GNSS information. While it is possible to estimate the self position using the high-precision positioning from the GNSS signal and automatically conduct agricultural tasks in the designated area of a field, there is a risk of collision with an obstacle since the surrounding area cannot be recognized by automated driving that is solely based on the GNSS signal. Obstacles are recognized using sensors such as lasers and radar for the autonomous travel of automobiles and robots. However, these sensors cannot identify the type of object, and the resulting robot mower cannot distinguish between grass and other obstacles during autonomous operations. Furthermore, high-precision GNSS positioning cannot be used in orchards and other places where satellite signals are blocked, rendering GNSS-based autonomous driving inoperable.

Herein, we develop a system for detecting obstacles and estimating the position of objects using image recognition. Obstacles in the environment are recognized using object detection with a convolutional neural network (CNN), the self position is estimated using Visual SLAM, and the obstacle avoidance is performed by combining the self-position and object detection information. A landmark with a known position is installed in the environment to improve the accuracy of the self-position estimation, with the self position corrected based on the landmark location.

2. MATERIALS AND METHODS

Herein, we combined the self-position estimation from Visual SLAM, object detection via deep learning, and obstacle avoidance from the path optimization Self-Position Estimation.

2.1 Hardware

2.1.1 Robot configuration

The robot that has been designed for this study is shown in Figure 1. The rear wheels are controlled by sending a signal from the motor driver. An embedded system is contained in the box, which is used for

environment recognition and route generation, with the driving commands sent from the embedded system to the motor driver.
Two cameras are used as the sensors and are mounted in the front and rear of the autonomous driving system on the assumption of round cutting. An inertial measurement unit is also mounted to the system to improve the accuracy of the self-position estimation.

Figure 1. Robot used in this study.

2.1.2 Camera

Intel Realsense D435 is used for depth camera (Figure 2). Realsense D435 comes with an RGB camera and two near-infrared cameras that capture depth images via stereo matching.

Figure 2. Realsense D435 depth camera.

2.1.3 Embedded system

Nvidia Jetson Xavier is used for the embedded system. Jetson Xavier is equipped with a graphics processing unit (GPU) and can be used for deep-learning applications.

2.2 Software

2.2.1 Self-position estimation

We use real-time appearance-based mapping (RTAB-map), which is a Visual SLAM library, to estimate the self position. The feature points are extracted from consecutive images in Visual SLAM, and the amount of movement between frames is estimated by matching the next image with feature points.

2.2.2 Obstacle and landmark detection

Yolo v3, which is an object detection algorithm with a CNN, is used for obstacle and landmark detection. Yolo v3 divides an image into grids and estimates the type of object and size of the bounding box for each grid. Here images of trees were collected from the Internet, and annotation data were manually created. Figure 3 illustrates this tree detection example using Yolo v3.

Figure 3. Tree detection example.

2.2.3 Position estimation of the object

Yolo v3 is used in conjunction with a CNN for the obstacle and landmark detection. The positions of the obstacles and landmarks are detected by the CNN, and the position of the detected object relative to the robot is estimated by associating the depth image with the detected position in the image. When an object is detected via the CNN, the distance is estimated by taking the center value of the distance, which corresponds to the pixel included in the detection position of the depth image, and the direction is estimated as the coordinate of the pixel in the center of the detection position and the camera parameter.

2.2.4 Obstacle avoidance path

Teb Local Planner is used for the avoidance route generation. The obstacle avoidance path is generated by rewarding the scheduled path and penalizing the obstacle to optimize the travel path. Examples of obstacle detection and an avoidance path are shown in Figure 4.

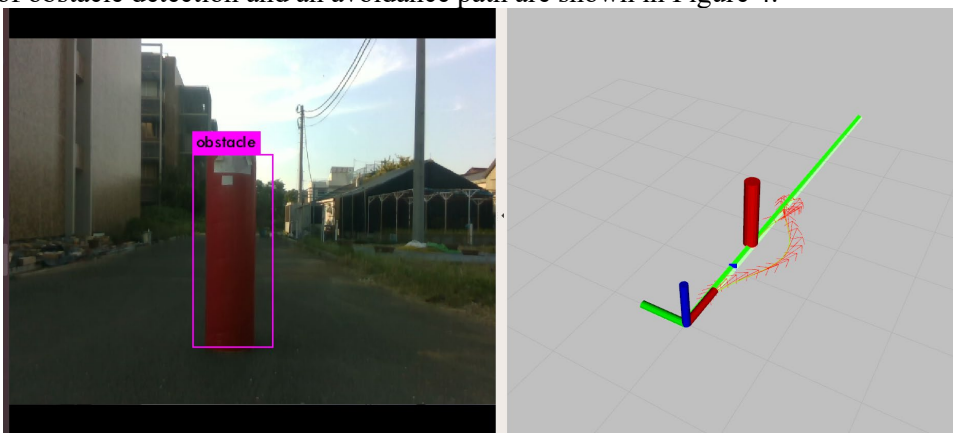

Figure 4. Examples of Obstacle Detection (left) and Avoidance (right).

2.2.5 Correcting the estimated position with a landmark observation

The drift of the estimated position is reduced by using the landmark in the CNN. The robot's position is estimated by observing a landmark with a known position. The self position is then corrected by adding the information on the estimated position to the appropriate node in the SLAM and adjusting the frame of reference accordingly.

3. EXPERIMENT

The experiment will be conducted at the Tanashi Experimental Forest, Graduate School of Agricultural and Life Sciences, the University of Tokyo. The accuracy evaluation of the self-position estimation will be performed by placing obstacles and landmarks in the test location, running the autonomous system in manual and autonomous mode, and measuring the true value using real-time kinematic (RTK)-GNSS.

4. ACKNOWLEDGMENT
This research was conducted with the support of the National Institute of Advanced Industrial Science and Technology Support Center "Innovative Technology Development, Emergency Development Project (including the Lead Project)".

REFERENCES
Annual Statistics of the Census of Agriculture and Forestry(1904–2015) (Translated from Japanese), Retrieved July 12, 2019, from https://www.e-stat.go.jp/stat-search/files?page=1&toukei=00500209&tstat=000001016170/
C. Rösmann, W. Feiten, T. Wösch, F. Hoffmann and T. Bertram. (2012), Trajectory modification considering dynamic constraints of autonomous robots. Proc. 7th German Conference on Robotics, pp 74-79
J. Redmon, S. Divvala, R. Girshick, and A. Farhadi. (2015), You only look once: Unified, real-time object detection. arXiv preprint arXiv:1506.02640.
M. Labbé and F. Michaud, (2018), "Long-term online multi-session graph-based SPLAM with memory management," in Autonomous Robots, vol. 42, 6, pp. 1133-1150
Noguchi, N. Barawid, (2011), O.J. Robot farming system using multiple robot tractors in Japan. Int. Fed. Autom. Control 2011, 18, pp633-637.
Sho Igarashi, Yutaka Kaizu, Kenji Imou, Toshio Tsutsumi, (2017), Development of autonomous riverside weeding robot (Translated from Japanese), Lecture Series of Automatic Control Association.60, pp52-53